JCB Journal of Cell Biology

ARTICLE

Pcp1/pericentrin controls the SPB number in fission yeast meiosis and ploidy homeostasis

Qian Zhu[1], Zhaodi Jiang[2], and Xiangwei He[1]

During sexual reproduction, the zygote must inherit exactly one centrosome (spindle pole body [SPB] in yeasts) from the gametes, which then duplicates and assembles a bipolar spindle that supports the subsequent cell division. Here, we show that in the fission yeast *Schizosaccharomyces pombe*, the fusion of SPBs from the gametes is blocked in polyploid zygotes. As a result, the polyploid zygotes cannot proliferate mitotically and frequently form supernumerary SPBs during subsequent meiosis, which leads to multipolar nuclear divisions and the generation of extra spores. The blockage of SPB fusion is caused by persistent SPB localization of Pcp1, which, in normal diploid zygotic meiosis, exhibits a dynamic association with the SPB. Artificially induced constitutive localization of Pcp1 on the SPB is sufficient to cause blockage of SPB fusion and formation of extra spores in diploids. Thus, Pcp1-dependent SPB quantity control is crucial for sexual reproduction and ploidy homeostasis in fission yeast.

Introduction

Eukaryotes typically have highly stable karyotypes, although adaptive changes—such as adding a whole set (or sets) of chromosomes to the genome, called polyploidization—are also seen, especially in the time scale of evolution. Extra set(s) of chromosomes are generally produced through whole-genome duplication or hybridization events (Albertin and Marullo, 2012; Otto, 2007). Additionally, polyploidy has long been considered to play a prominent role in the process of evolution (Otto and Whitton, 2000). Evidence strongly suggests that the budding yeast *Saccharomyces cerevisiae* doubled its entire genome and reassembled it during evolution (Wolfe and Shields, 1997). For this unicellular fungus, polyploidy occurs easily either naturally or artificially (Querol and Bond, 2009). Moreover, its polyploids are mitotically stable, although genome instability does increase in conjunction with increasing ploidy, with the mechanisms poorly understood (Mayer and Aguilera, 1990). In contrast, for *Schizosaccharomyces pombe*, polyploids have not been seen in natural isolates and are difficult to construct in the laboratory, for unknown reasons (Molnar and Sipiczki, 1993).

Centrosomes are the major microtubule organizing centers (MTOCs) in animal cells, whereas their functional counterpart in yeasts is the spindle pole body (SPB; Bettencourt-Dias and Glover, 2007; Kilmartin, 2014). For both centrosomes and SPBs, their quantities are tightly controlled to ensure that a bipolar spindle is assembled which segregates chromosomes accurately in mitosis and meiosis (Basto et al., 2008; Ganem et al., 2009; Ohta et al., 2012; Rüthnick and Schiebel, 2016). In particular, during sexual reproduction, to ensure that the zygote possesses only one centrosome (SPB) at the entry of nuclear division, the centrosomes (SPBs) of both gametes fuse to form the zygote's first centrosome (SPB), which then duplicates and assembles a bipolar spindle to support the first cell division. It is generally thought that, for most metazoans, the centrosome of the zygote is assembled from the centriole provided by the male gamete and pericentriolar material (PCM) provided by the female gamete (Schatten, 1994). To this end, the centrosomes of gametes undergo a series of transmutations during gametogenesis, which includes "centrosome reduction" (various degrees of loss of microtubule nucleation function and loss of PCM) during spermiogenesis, and the elimination or inactivation of centrioles during oogenesis (Manandhar et al., 2005; Mikeladze-Dvali et al., 2012; Pimenta-Marques et al., 2016; Schatten, 1994). Defects in centrosome degeneration during gametogenesis will affect the number and function of the centrosome in the zygote, leading to aberrant embryo development.

For sexual reproduction in yeast, haploid gametes of different mating types cross to form a diploid zygote, which then undergoes meiosis and produces four haploid spores. In general, after conjugation, the two nuclei are pulled together by cytoplasmic microtubules and fuse to form a diploid nucleus. The

[1]The Ministry of Education Key Laboratory of Biosystems Homeostasis and Protection and Innovation Center for Cell Signaling Network, Life Sciences Institute, Zhejiang University, Hangzhou, China; [2]National Institute of Biological Sciences, Beijing, China.

Correspondence to Xiangwei He: xhe@zju.edu.cn.

two SPBs from both mating partners also fuse to form a diploid SPB in a larger size to support the subsequent meiotic cell divisions (or mitotic divisions when ample nutrients are supplied immediately after conjugation; Melloy et al., 2007; Tange et al., 1998). The SPBs derived from the mating partners are theoretically identical. Little is known about the regulation of SPB fusion and any specific conditions that may be required for SPB fusion, such as whether the SPBs undergo any prior transmutation.

Pcp1 is the fission yeast orthologue of the mammalian pericentrin, a key centrosomal PCM component that performs conserved functions in recruiting the γ-tubulin complex for nucleating microtubule polymerization (Fong et al., 2010; Lin et al., 2015). Pcp1 is constantly localized to SPB during mitotic growth, whereas in the early stage of meiosis, it dissociates from SPB and does not reassociate with the SPB until the onset of meiosis I (MI; Ohta et al., 2012). However, the potential significance of this sexual differentiation–specific dynamic localization is poorly understood. Although yeasts do not have a centriole, Pcp1 can interact with and recruit the exogenously expressed centriole component, SAS-6, through its PACT (pericentrin/AKAP450 centrosomal targeting) domain. This conserved SAS-6–pericentrin interaction is important for centriole assembly in animal cells (Ito et al., 2019). This indicates that the conservation of the function of PCM modules is beyond their structural preservation. Various studies together have indicated that Pcp1 (pericentrin) is important for the quantity control of SPBs (centrosomes). Overexpression of Pcp1 in *S. pombe* or pericentrin in animal cells leads to the formation of supernumerary SPBs and extra centrioles, respectively (Flory et al., 2002; Jin et al., 2005; Loncarek et al., 2008). Moreover, both overexpression of pericentrin and centrosome amplification are hallmarks of many cancers. The degree of centrosomal aberrations closely correlates with chromosome instability and malignancy of tumors (Leber et al., 2010; Lingle et al., 1998; Pihan et al., 2001).

Meiosis (generally referring to diploid meiosis) is characterized by one round of DNA replication followed by two consecutive rounds of nuclear divisions, producing four haploid gametes. Polyploid meiosis, especially with odd number sets of chromosomes, is less likely to execute accurate chromosome segregation because of abnormal homologous chromosome pairing and often leads to the production of aneuploid gametes with low viability (Grandont et al., 2013; Niwa and Yanagida, 1985; St. Charles et al., 2010; Tel-Zur et al., 2005). In this study, we found a new characteristic of polyploid (triploid and tetraploid) meiosis in *S. pombe*: the production of asci containing more than four spores due to dysregulation of SPB number. We show that in polyploid zygotes, the fusion of SPBs is blocked by the persistent localization of Pcp1 on the SPB, leading to the formation of supernumerary SPBs, which in turn leads to the assembly of multipolar spindles and the eventual formation of extra-spored asci. Thus, the role of the dynamic regulation of PCM modules for centrosome (SPB) inheritance during sexual reproduction is conserved from yeast to metazoans. Furthermore, we provide evidence suggesting that SPB quantity control may be a key factor limiting the increase of ploidy in *S. pombe*.

Results

S. pombe polyploid zygotic meiosis produces extra spores

In *S. pombe*, diploids can be formed by fusing haploids of opposite mating types (h^+ and h^-) when nutrients are scarce, a process called sexual conjugation (Sipiczki, 1988). Although these diploids (h^+/h^-) can proliferate mitotically with ample nutrient supplies, they stop mitotic growth and switch to meiosis mode to produce spores once nutrients are scarce again and thus are called sporulating diploids (Egel and Egel-Mitani, 1974). In contrast, stable, nonsporulating diploids that are homozygous in mating type can be formed occasionally by endoreduplication, a process in which the cells skip the cytokinesis after DNA replication and enter a new round of replication (Edgar and Orr-Weaver, 2001), or by artificial protoplast fusion in the laboratory (Sipiczki and Ferenczy, 1977). These nonsporulating diploids (h^+/h^+ or h^-/h^-) are unable to undergo meiosis on their own but are capable of conjugating with a haploid or another diploid of the opposite mating type, undergoing triploid or tetraploid meiosis, respectively (Gutz, 1967; Niwa and Yanagida, 1985).

We obtained nonsporulating diploid strains from the transformants of the classic yeast lithium acetate DNA transformation method. These diploids were obtained in a relatively high frequency (~3–10%), regardless of the DNA used for transformation, possibly due to an endoreduplication event or due to the inclusion of polyethylene glycol in the experimental procedure that promotes cell fusion (Harari et al., 2018). These strains could be propagated successfully with a stable diploid karyotype and grew equally as well as their haploid precursors (Fig. S1, A–C). However, we noticed not only that the triploid meiosis resulting from the mating of the nonsporulating diploid and a haploid produced spores with low viability but also that a large percentage of triploid asci contained more than four, up to eight, spores (Fig. 1, A and B).

This supernumerical spore meiosis is reminiscent of the "twin meiosis" described in tetraploid meiosis, in which diploid cells of opposite mating types conjugate but do not undergo nuclear fusion after plasmogamy. Instead, the two nuclei undergo meiosis independently, ultimately forming asci with eight spores (Gutz, 1967). To validate whether the supernumerical spore meiosis that we observed was twin meiosis, the process of triploid zygotic meiosis was microscopically examined. In the two cells involved in the mating, chromosome I of one of the cells was marked with GFP at the *lys1* locus near the centromere (*lys1*-GFP), whereas chromosome II of the other cell was marked with tdTomato at the centromere (*cnt2*-tdTomato; Sakuno et al., 2009; Sakuno et al., 2011), so that the motion of these two individual chromosomes could be tracked microscopically during meiosis. As shown in Fig. 1 C, only one elongated, horsetail-shaped nucleus was observed in the triploid zygotes during meiotic prophase. This horsetail nucleus contained both tagged chromosomes originating from the two mating partners (Fig. 1 C), demonstrating successful occurrence of nuclear fusion in contrast to the two independent nuclei characteristic of twin meiosis. To test whether this discrepancy is due to the difference between a triploid meiosis in our study and the previously reported tetraploid meiosis, we also performed a tetraploid meiosis (crossing between two nonsporulating diploids).

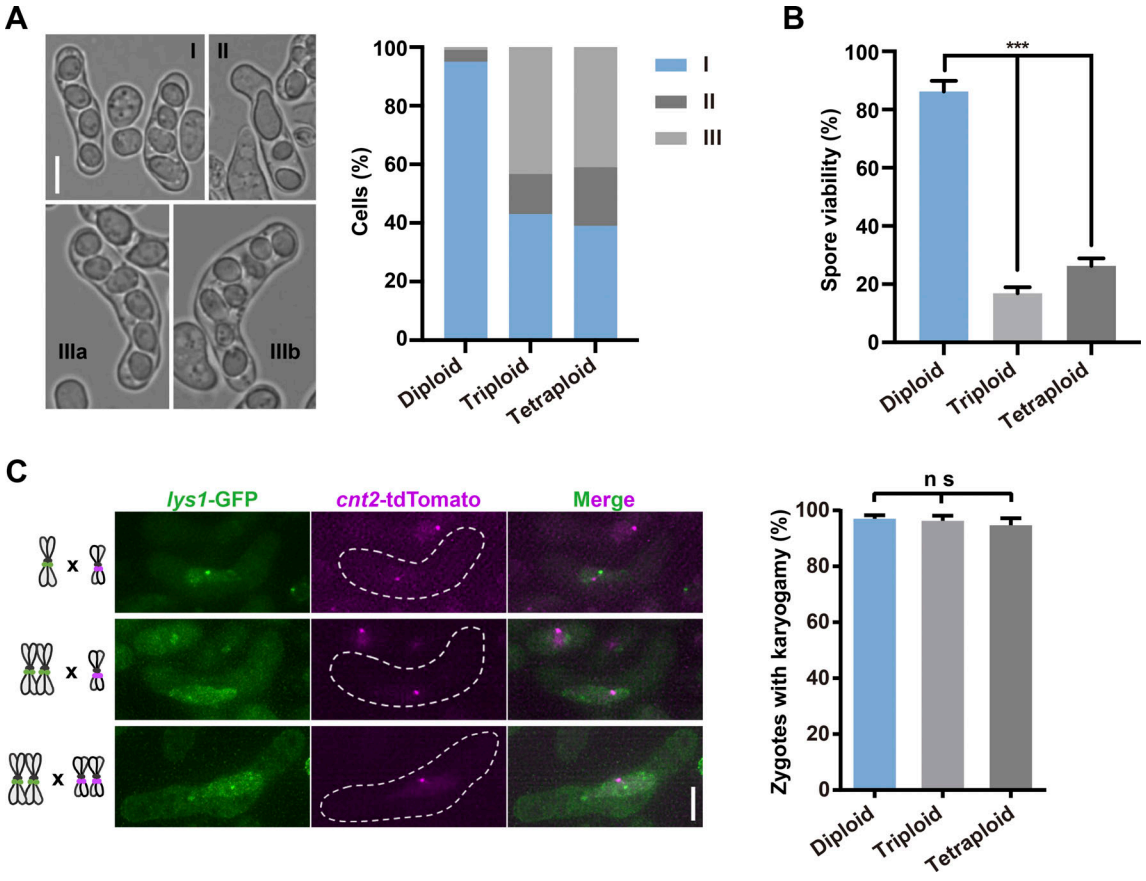

Figure 1. **Polyploid zygotic meiosis produces extra spores. (A)** Representative microscopic images of asci with different numbers of spores (left). Quantification of shown phenotypes (left) of asci of different ploidy (right). I, asci with four spores; II, asci with less than four spores; IIIa and IIIb, asci with more than four spores. $n \geq 200$ cells for each. **(B)** Quantification of spore viability from zygotic meiosis of different ploidy. Error bars represent SD; ***, $P < 0.001$ (one-way ANOVA). **(C)** Microscopic images of zygotes with different ploidy marked by *lys1*-GFP and *cnt2*-tdTomato during meiotic prophase (left panels). Quantification of zygotes with karyogamy (right panels). Error bars are SDs from three independent experiments ($n \geq 200$ cells each; one-way ANOVA). Scale bars in A and C, 5 µm.

Consistently, a single horsetail nucleus containing chromosomes from both gametes was observed (Fig. 1 C).

These results together indicate a novel mechanism different from twin meiosis for producing extra spores in polyploid meiosis.

Formation of supernumerary SPBs and multipolar spindles in polyploid zygotic meiosis

Another plausible mechanism for the formation of extra spores is an extra round of postmeiotic (or MIII-like) nuclear division (Molnar and Sipiczki, 1993; Tanaka and Hirata, 1982; Widra and De Lamater, 1954). In *S. pombe* and *S. cerevisiae*, mutants with perturbed meiosis exit undergo an MIII-like division leading to the formation of additional (more than four) daughter nuclei, such as mutants that are defective in anaphase-promoting complex/cyclosome activators (Aoi et al., 2013; Wang et al., 2020). To determine whether this was the case in polyploid meiosis, we performed time-lapse microscopy, monitoring the dynamics of microtubules by tagging tubulin with GFP (GFP-Atb2) and chromosome segregation by tagging histone H3 with mCherry (Hht1-mCherry) in polyploid zygotes (Ding et al., 1998). No MIII-like nuclear division was detected in any complete triploid or tetraploid meiosis events we observed ($n > 100$). In contrast, instead of one or two rod-shaped bipolar spindles organized at MI and MII, respectively, as seen in normal diploid meiosis (Fig. 2 A), multipolar (mostly tripolar) spindles were frequently formed at both MI and MII of the polyploid zygotes (Fig. 2 B; and Fig. S2, A and B). The multipolar spindles often led to a multipolar nuclear division or an uneven bipolar nuclear division, resulting in the formation of extra daughter nuclei (Fig. 2 B; and Fig. S2, A and B).

The formation of multipolar spindles indicated the presence of supernumerary MTOCs-SPBs. Indeed, by marking SPB with GFP-labeled SPB component protein Sad1 (Hagan and Yanagida, 1995), supernumerary SPBs were observed in the polyploid zygotes, usually at the poles of the multipolar spindles (Fig. 2, C–E; and Fig. S2, C and D). Electron microscopic (EM) examination showed that there were no obvious defects in the architecture and morphology of SPBs during triploid and tetraploid meiotic nuclear division, and the SPBs were competent in nucleating spindle microtubules (Fig. 2 F and Fig. S2 E). In addition, a component of the SPB half-bridge, Sfi1, which is necessary for SPB duplication (Kilmartin, 2003; Lee et al., 2014), was also colocalized with the extra Sad1 foci (Fig. S2 F). This observation

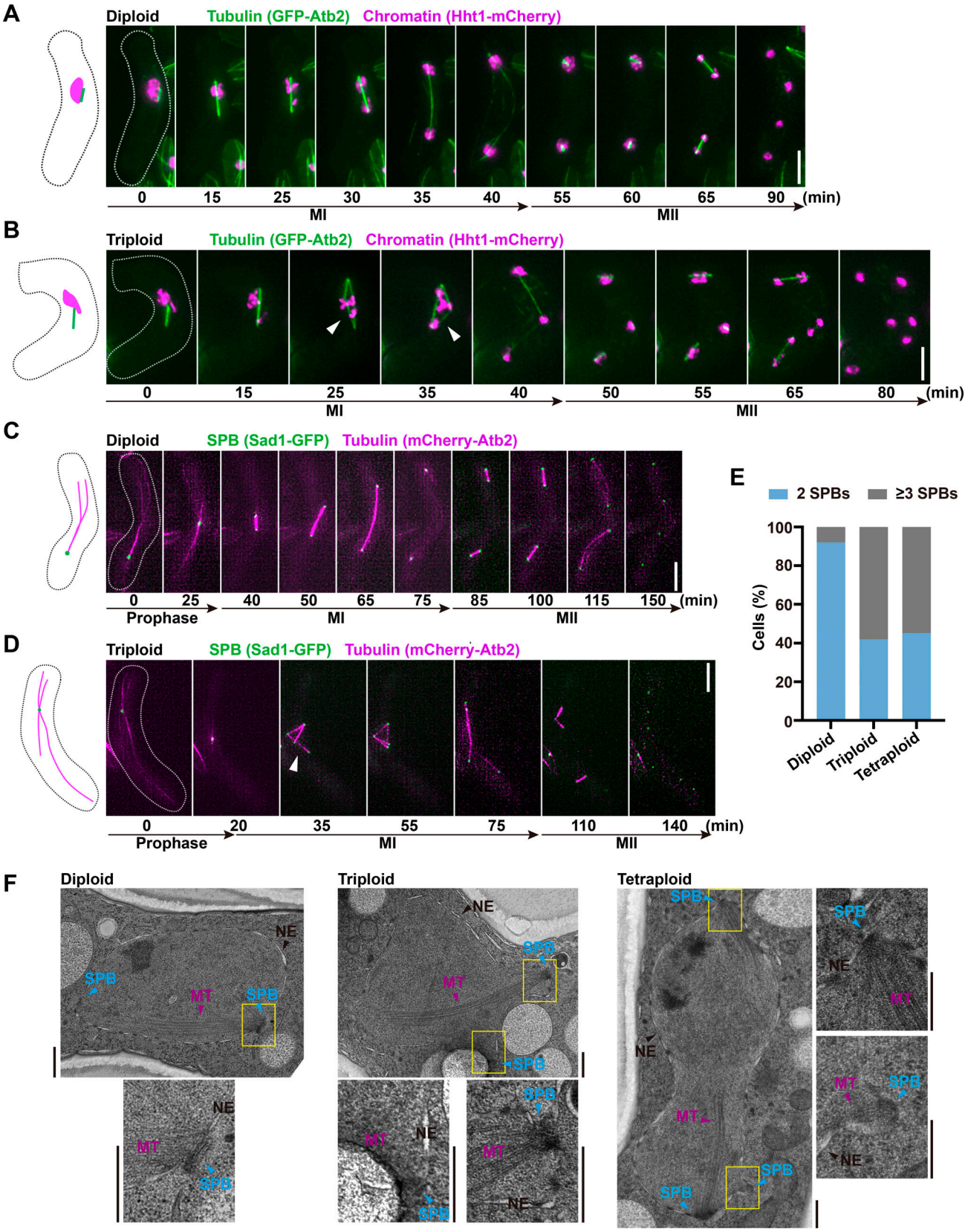

Figure 2. **Polyploid zygotic meiosis undergoes multipolar nuclear division. (A and B)** Representative time-lapse images of diploid (A) and triploid (B) zygotes expressing GFP-Atb2 (microtubules) and Hht1-mCherry (chromatins). Multipolar spindles are indicated (arrowheads). Scale bars, 5 µm. **(C and D)** Representative time-lapse images of diploid (C) and triploid (D) zygotes expressing Sad1-GFP (SPB) and mCherry-Atb2 (microtubules). Arrowhead indicates a multipolar spindle with supernumerary SPBs in the triploid zygote. Time 0 is an arbitrary time point in meiotic prophase. Scale bars, 5 µm. **(E)** Quantification of zygotes of different ploidy with extra SPBs at MI. $n \geq 200$ cells for each. **(F)** Transmission electron micrographs of MI nuclei in diploid, triploid, and tetraploid zygotes. The boxed regions are magnified below or to the right. Scale bars, 500 nm. MT, microtubule.

further indicates that the extra SPBs retain a relatively intact structure and function, in agreement with their ability to duplicate and assemble multipolar or extra bipolar spindles at MII.

These results demonstrate that polyploid zygotes are defective in SPB quantity control, leading to the assembly of multipolar spindles and inaccurate chromosome segregation.

Loss of dynamic localization of Pcp1 on the SPB in polyploid zygotes

When *S. pombe* is committed to sexual differentiation, key components of the SPB exhibit distinct, dynamic patterns of association with the SPB in a cell cycle stage-specific manner, in contrast to mitosis, in which these components are constantly localized on the SPB throughout the cell cycle. There are roughly two groups: (1) those that are stably associated with the SPB throughout the sexual reproduction cycle, including the core scaffold proteins Ppc89 and Sid4, the half-bridge proteins Sfi1 and Cdc31, and the linker of nucleoskeleton and cytoskeleton complex component Sad1 (Bestul et al., 2017; Ohta et al., 2012); and (2) those that are associated with the SPB dynamically in the early stages of sexual differentiation, including Pcp1, Cut12, and Hrs1. Pcp1 and Cut12 are disassociated from the SPBs before SPB fusion and throughout meiotic prophase and relocate to the SPB at the start of MI (Ohta et al., 2012), whereas Hrs1, a meiosis-specific protein important for nuclear oscillation, is localized on the SPB specifically in prophase and disassociated from SPB at the onset of MI (Saito et al., 2005; Tanaka et al., 2005).

To explore whether the defective quantity control of SPB in polyploid meiosis is related to the specific dynamic localization of SPB components, we monitored the dynamics of various SPB components at the early stage of sexual differentiation. First, we found that those components that have been shown not to change dynamically were indeed inflexible in their SPB localization in both diploid and polyploid meiosis, as exemplified by the dynamics of Ppc89 in a diploid zygote. By tagging Ppc89 with GFP in one of the gametes and with mCherry in another, we observed that the two SPB dots maintained their original color for a substantial period of time after plasmogamy until the SPBs fused to form a single fluorescent dot (Fig. 3 A). This indicates that no detectable exchange or dissociation of Ppc89 molecules from SPB occurred before SPB fusion. Additionally, as shown in a previous study (Ohta et al., 2012), Ppc89 remained associated with the SPB throughout meiotic prophase after SPB fusion (using stage-specific localization of Hrs1-mCherry on the SPB as a marker for prophase; Fig. 3 B).

In contrast, Pcp1, which exhibited a dynamic association with the SPB during diploid zygotic meiosis (Ohta et al., 2012), lost its dynamics in polyploid zygotes. In diploid zygotes, Pcp1 had disappeared from the SPB when the signal of Hrs1 appeared (Fig. 3 C). During triploid zygotic meiosis, however, in ∼50% of zygotes, Pcp1-GFP persisted at the SPB at the stage in which Hrs1-mCherry appeared on the SPB (Fig. 3, D and E). Moreover, the undissociated Pcp1 was apparently due to the specific, persistent Pcp1 localization on the diploid-originated SPB, which could be seen by tagging Pcp1 in the diploid and haploid mating partners with GFP and mCherry, respectively. After conjugation, the Pcp1-GFP dot from the diploid persisted, whereas the Pcp1-mCherry dot from the haploid disappeared (Fig. S3 A). This persistent localization of Pcp1 in meiotic prophase was also observed in tetraploid zygotes (Fig. S3, A and B).

However, the dynamics of Cut12 association with the SPB in polyploid zygotes was no different from that in diploid zygotes, although Cut12 and Pcp1 exhibited the same dynamic pattern of SPB association in diploid zygotic meiosis (Fig. S3, C and D). In addition, previous works have shown that the Polo kinase/Plo1, which executes multiple roles on the SPB, is also excluded from SPB during meiotic prophase and that its restoration on the SPB is required for relocalization of both Pcp1 and Cut12 upon entry into MI (Krapp et al., 2010; Ohta et al., 2012). We monitored the localization of Plo1 in polyploid zygotes. Similar to Cut12, Plo1 was not localized to the SPB during meiotic prophase in both polyploid and diploid zygotes, but it was localized at kinetochores, as previously observed (Fig. 3 F and Fig. S3 E; Krapp et al., 2010). This finding suggests that the persistence of Pcp1 on the SPB in polyploid zygotes is independent of the enrichment of Plo1 on the SPB. Collectively, we conclude that the dynamics of Pcp1 on the SPB is specifically perturbed in polyploid zygotes.

Constitutive localization of Pcp1 on the SPB causes the formation of extra spores in diploid zygotic meiosis

We speculated that the loss of the dynamics of association with the SPB of Pcp1 might be a causal factor for extra-spored asci formation in polyploid meiosis. To test this, we asked whether forcing persistent Pcp1 localization on the SPB was sufficient to induce these phenotypes in an otherwise diploid meiosis. To this end, we constructed a Pcp1–Ppc89–GFP fusion expressed under the endogenous promoter of *pcp1*, so that the expression time and expression level of Pcp1 remained WT-like. In this fusion construct, the relative orientation of Pcp1 and Ppc89 matches their original localization on the SPB: that is, Ppc89, through its N terminus, interacts with the C terminus of Pcp1 (Fig. 4 A; Bestul et al., 2017). During the mating between the haploid cells carrying the fusion protein, Pcp1–Ppc89–GFP indeed persisted on the SPB throughout meiotic prophase (Fig. 4 B), mimicking the persistence of Pcp1 on the SPB in the polyploid zygotes. Importantly, the fusion construct exerted a dominant effect in producing asci with extra spores in diploids (Fig. 4, C and D). After a diploid meiosis with one of the mating partners carrying the fusion (unilateral cross), ∼30% of asci were found to contain more than four spores; meanwhile, with both mating partners carrying the fusion protein (bilateral cross), up to 80% of asci contained extra spores (Fig. 4 D).

Moreover, meiosis of diploid zygotes with persistent Pcp1–SPB association was accompanied by the formation of supernumerary SPBs and the assembly of multipolar spindles (Fig. 4 D and Fig. S4 A). However, in contrast to meiosis, mitosis in cells expressing Pcp1–Ppc89–GFP was normal, with no extra SPBs or multipolar spindle formation (Fig. S4, B and C), suggesting that the fusion protein did not interfere with the SPB's functions in mitotic proliferation and that the extra SPBs caused by constitutive Pcp1–SPB association was meiosis specific. Furthermore, consistent with the fact that the dynamics of Cut12 remained unchanged in polyploid meiosis (Fig. S3, C and D), the Cut12–Ppc89–GFP fusion

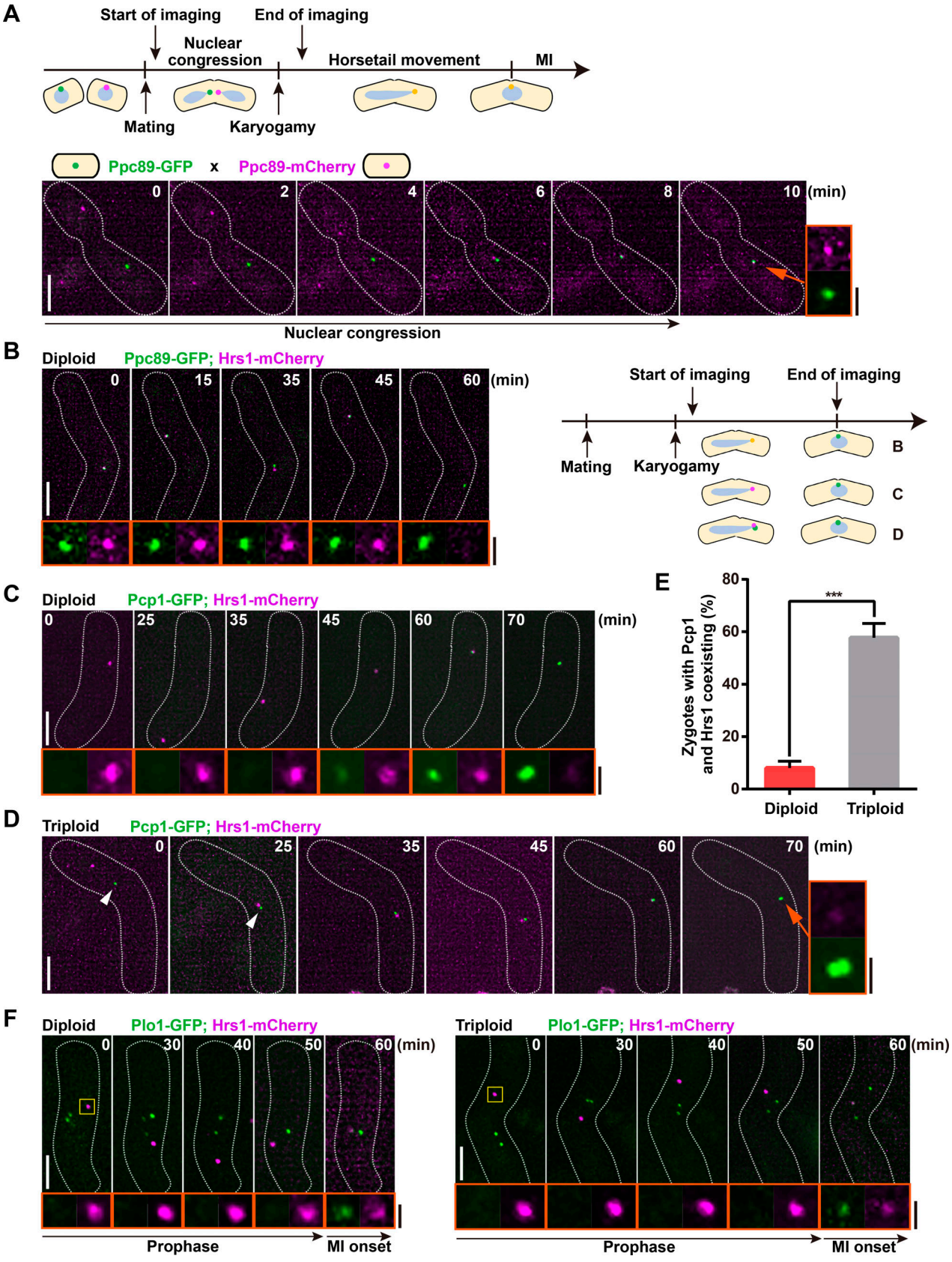

Figure 3. **Dynamics of Pcp1 association with the SPB is lost in polyploid zygotes. (A)** Time-lapse images of zygotes from mating between two haploid gametes expressing Ppc89-GFP and Ppc89-mCherry, respectively. Schematic shows the zygotic meiosis process and indicates the beginning and end of microscopic imaging. Inset is an enlargement of the indicated SPB dot. Scale bars: white, 5 µm; black, 1 µm. **(B and C)** Representative time-lapse images of

meiotic prophase in diploid zygotes expressing Ppc89-GFP and Hrs1-mCherry (B) or Pcp1-GFP and Hrs1-mCherry (C). A schematic shows the corresponding meiosis process (B, right panels). **(D)** Representative time-lapse images of prophase in triploid zygotes expressing Pcp1-GFP and Hrs1-mCherry. Arrowheads point to Pcp1 dots persisting on SPBs throughout prophase. **(E)** Percentage of zygotes with Pcp1-GFP and Hrs1-mCherry dots coexisting during prophase. Note that even during normal diploid meiosis, in the transition from prophase to MI, there is a short period of time when Pcp1 and Hrs1 are colocated on the SPB, as shown in C at 60 min, which is included in the statistics. Error bars are SDs from three independent experiments ($n \geq 150$ cells each). ***, $P < 0.001$ (two-tailed *t* test). **(F)** Time-lapse images of meiotic prophase in diploid (left panels) and triploid (right panels) zygotes expressing Plo1-GFP and Hrs1-mCherry. In B–D and F, time 0 is an arbitrary time point in early meiotic prophase. Insets are enlargements of the corresponding SPB dots. Scale bars: white, 5 µm; black, 1 µm.

protein constructed by the same strategy did not cause the formation of extra spores in diploid zygotic meiosis (Fig. S4, D and E).

To further verify the role of the dynamic localization of Pcp1 on sporulation, we introduced two previously identified temperature-sensitive *pcp1* mutation alleles, *pcp1-14* and *pcp1-15*, into the Pcp1–Ppc89–GFP fusion construct to specifically compromise the biological activities of Pcp1 (Tang et al., 2019). Between the two mutants, *pcp1-14* shows stronger defects with noticeable reduction in Pcp1 protein levels even under the permissive condition (27°C) and progressive reduction in protein levels with elevating temperature (Tang et al., 2014), whereas *pcp1-15* mutant is defective in recruiting γ-tubulin complex to the SPB, thus exhibiting compromised activities of nucleating microtubules (Fong et al., 2010). Consistently, formation of extra spores caused by forced Pcp1–SPB association was significantly attenuated in both *pcp1* mutants even at 29°C (Fig. 4, E and F). This result suggests that either the protein level or the functional integrity of Pcp1 that persistently localized on the SPB specifically has an impact on its subsequent interference with SPB quantity control.

In addition to identifying Pcp1 as a specific element in controlling SPB number, the results above also suggest that the defect of SPB quantity control may reside specifically on the SPB before meiosis entry; in other words, before karyogamy, which is needed to reduce SPB number from two to one by SPB fusion. To test this, we reasoned that bypassing the requirement of karyogamy in azygotic meiosis (i.e., meiosis process initiated in a sporulating diploid cell directly, without the nuclear fusion step of zygotic meiosis that involves the mating of two gametes) would rescue the defects of extra SPBs and the low success rate of meiosis overall. Indeed, when the sporulating diploid cells (h^+/h^-) expressing Pcp1–Ppc89–GFP were induced to undergo meiosis, the resulting azygotic asci appeared normal, and almost all of them contained four spores, despite the fact that Pcp1–Ppc89–GFP had a persistent localization on SPBs as in zygotic meiosis (Fig. 4 G). This is different from the result of artificially tethering Plo1 to SPB during meiotic prophase, which would result in the formation of extra spores in both zygotic and azygotic meiosis due to overduplication of SPBs (Fig. S4 F; Ohta et al., 2012).

Dissociation of Pcp1 from SPB during mating is required for SPB fusion

We sought to investigate how loss of dynamics in SPB localization of Pcp1 might lead to SPB number dysregulation. As described above, persistent Pcp1–SPB association only affected zygotic sporulation but not azygotic sporulation (Fig. 4, C and G), a phenomenon that is common in mutants specifically affecting karyogamy. Karyogamy is a prerequisite process for zygotic meiosis, including major steps of nuclear congression, fusion of nuclear envelopes (NEs), and fusion of SPBs (Kurihara et al., 1994; Nishikawa et al., 2008). The mutants that specifically affect zygotic sporulation involve genes that affect nuclear congression, such as *mal3* and *mto1* (Polakova et al., 2014), and genes that affect fusion of NEs, such as *tht1* (Tange et al., 1998).

During prophase of triploid and tetraploid zygotic meiosis, as well as diploid zygotic meiosis with artificial Pcp1 fixation on the SPB, only a single horsetail nucleus was observed (Fig. 1 C and Fig. 5 A), suggesting that nuclear congression or NE fusion was not perturbed in these zygotes. We thus postulated that the dissociation of Pcp1 from SPB might be specifically responsible for the fusion of SPBs during karyogamy. Indeed, supporting this notion, in diploid zygotes with artificially undissociated Pcp1, two distinct, side-by-side GFP spots were frequently observed (23% compared with ∼1% in WT zygotes) at the tip of a single horsetail nucleus (Fig. 5 A). In comparison, at the corresponding stage of WT diploid zygotes, a single SPB formed by the fusion of two SPBs was microscopically detected as a single GFP spot at the tip of the horsetail (Fig. 5 A; Tange et al., 1998). Thus, in diploid zygotes with persistent Pcp1 association with SPBs, the SPBs were brought together by cytoplasmic astral microtubules, but the fusion step was blocked.

To further clarify this SPB fusion blocking in polyploid zygotes, we monitored the process of polyploid meiosis in the genetic background of *tht1Δ*. Loss of function of Tht1 affects fusion of NEs, producing zygotes containing two unfused, juxtaposed horsetail nuclei that oscillated, dragged together by a single SPB (Tange et al., 1998). We predicted that further perturbation of SPB fusion in *tht1Δ* zygotes would result in a twin meiosis–like division because the two nuclei would be brought together but without both nuclear membrane fusion and SPB fusion and thereby would proceed with meiosis separately. As a control, in *tht1Δ* diploid zygotes, as shown in previous studies, two unfused horsetail nuclei were pulled by one unified SPB during prophase. Upon entry into MI, due to the severe nuclear fusion defects, a variety of chromosomal segregation abnormalities occurred (Fig. 5 B and Fig. S5 A). Strikingly, we observed that among these defects, a high percentage of zygotes (∼40%) showed that the two duplicated SPBs moved along the nuclear membrane of only one of the two nuclei and mediated the segregation of chromosomes in this nucleus, whereas the other nucleus lost all SPBs and remained in the middle of the zygotes until the end of meiosis (Fig. 5 B). This result explains the previous observation of large nuclei without spore wall encapsulation in *tht1* mutant asci, because spore wall formation is initiated on the modified SPB (Tange et al., 1998).

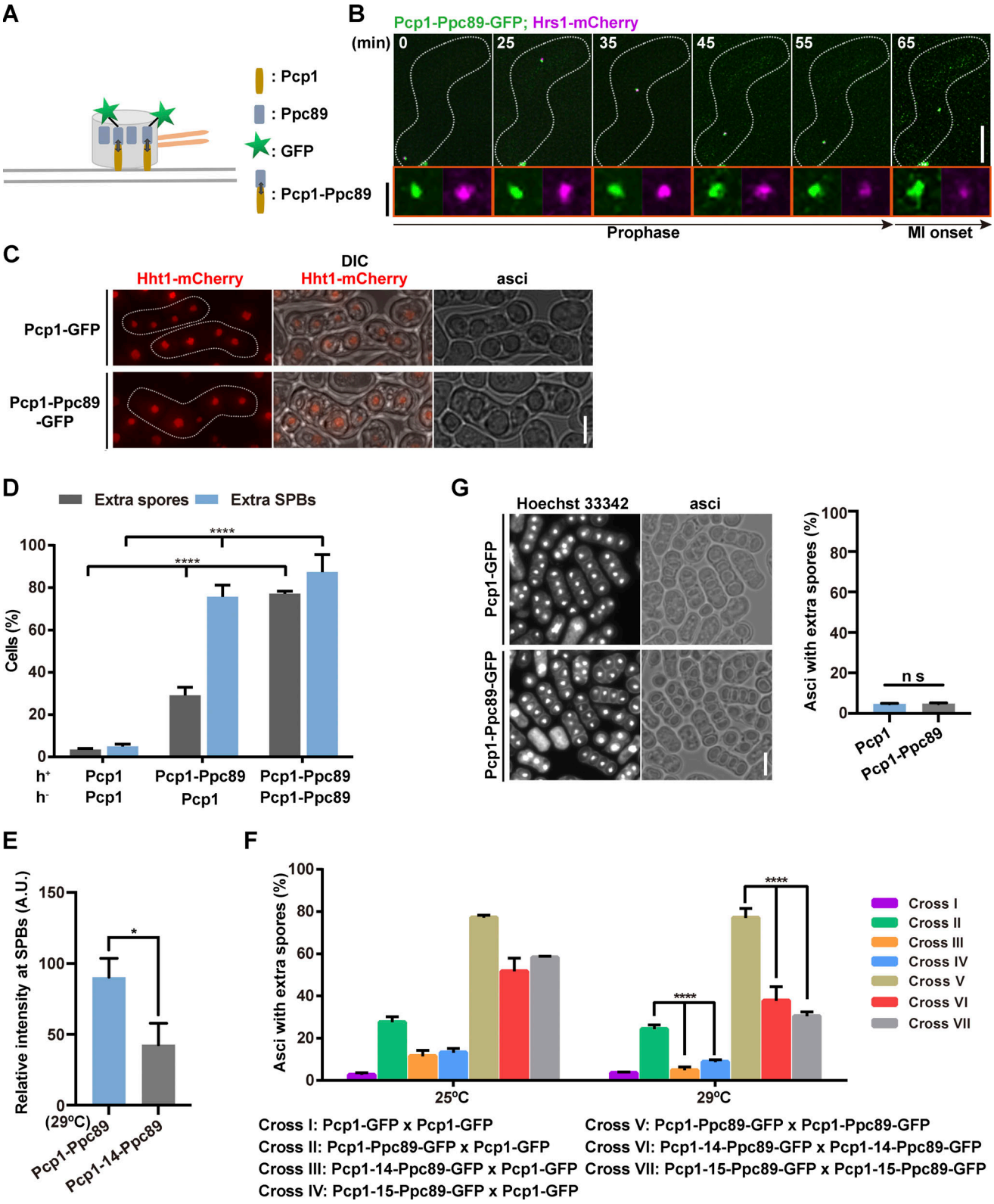

Figure 4. **Persistent localization of Pcp1 on the SPB in diploid zygotes mimics the phenotype of polyploid meiosis. (A)** Schematic of SPB with Pcp1–Ppc89–GFP fusion construct. **(B)** Representative time-lapse images of diploid zygotes expressing Pcp1–Ppc89–GFP and Hrs1-mCherry. Insets are enlargements of the corresponding SPB dots. Scale bars: white, 5 µm; black, 1 µm. **(C)** Microscopic images of asci expressing Hht1-mCherry (chromatins) with or without constitutive Pcp1–SPB association. **(D)** Quantification of cells with supernumerary SPBs and extra spores in the indicated crosses. Pcp1, Pcp1-GFP; Pcp1-Pcpc89, Pcp1–Ppc89–GFP. Error bars are SDs from three independent experiments ($n \geq 200$ cells each). ****, $P < 0.0001$ (one-way ANOVA). **(E)** Quantification of GFP fluorescence signal on SPBs during meiotic prophase in zygotes expressing Pcp1–Ppc89–GFP or Pcp1–14-Ppc89–GFP at 29°C. Error bars are SDs from three independent experiments ($n \geq 50$ cells each). *, $P < 0.05$ (two-tailed t test). **(F)** Percentage of asci containing extra spores in the

indicated crosses. Error bars are SDs from three independent experiments ($n \geq 200$ cells each). ****, $P < 0.0001$ (two-way ANOVA with Šidák's multiple comparisons test). **(G)** Microscopic images of azygotic asci stained by Hoechst 33342 expressing Pcp1-GFP or Pcp1–Ppc89–GFP (left). Quantification of azygotic asci containing extra spores (right). Sporulating diploids expressing Pcp1-GFP or Pcp1–Ppc89–GFP were transferred to nutrient-scarce ME medium to induce azygotic meiosis and sporulation. Error bars are SDs from three independent experiments ($n \geq 200$ cells each; two-tailed *t* test). Scale bars in C and G, 5 µm.

However, in *tht1Δ* polyploid zygotes, the two unfused horsetail nuclei were often seen either oscillating separately with a single SPB or oscillating in parallel because they were pulled by two adjoining SPBs (Fig. S5 B). Moreover, in *tht1Δ* triploid or tetraploid zygotes, often both unfused nuclei conducted meiosis separately, each with a pair of SPBs, akin to a twin meiosis division, resulting in asci containing eight spores (Fig. 5, C and D; and Fig. S5 C). Remarkably, spore viability of polyploid meiosis was significantly restored by *tht1Δ*, especially in tetraploids with two complete sets of chromosomes (Fig. 5 E). This suggests that defects in polyploid meiosis can be bypassed, at least partially, by twin meiosis in which neither SPB fusion nor NE fusion occurs. This mimics the phenotype of twin meiosis in tetraploid zygotes observed in a previous study (Gutz, 1967), suggesting that the genetic background of the strains or certain experimental conditions used in the study decades ago might specifically affect the execution of karyogamy. In addition, *tht1*$^{+}$ deletion significantly increased the percentage of zygotes with extra SPBs compared with WT even in diploid zygotes (Fig. 5 F and Fig. S5 D). This observation suggests that in the process of karyogamy, the fusion of the NE might facilitate the completion of SPB fusion.

The results above indicate that the failure of Pcp1 to dissociate from SPB will lead to the blockage of SPB fusion, which may be the key to the formation of supernumerary SPBs and extra spores in subsequent polyploid meiosis. Moreover, in line with this conclusion, the zygotes derived from the mating of cells expressing Pcp1-Ppc89-GFP could not return to or maintain stable mitotic growth with restored nutritional supplies. Those cells that returned to mitosis still possessed extra SPBs and exhibited severe mitotic defects during subsequent vegetative growth (Fig. S5 E).

Defects in homologous chromosome pairing enhance spindle multipolarity

Although the constitutive localization of Pcp1 on the SPB in diploid zygotes categorically mimicked both phenotypes of extra SPBs and extra spores in polyploid meiosis, we noticed a quantitative discrepancy. In diploid zygotic meiosis with persistent Pcp1–SPB association, although a high percentage of zygotes formed extra SPBs at MI, fewer asci contained extra spores at the final stage. This quantitative discrepancy was especially noticeable for the unilateral mating in which only one of the gametes carried Pcp1–Ppc89–GFP (~30% for extra spore formation versus ~80% for extra SPB formation; Fig. 4 D). In contrast, for polyploid zygotic meiosis, the percentage of zygotes with extra SPBs was approximately the same as that of resulting extra-spored asci (~50% for both extra spore formation and extra SPB formation; Fig. 1 A and Fig. 2 E). These observations raised the question of why not all supernumerary SPBs led to formation of extra spores in diploid zygotes. To address this paradox, we monitored the motion dynamics of microtubules and SPBs in the diploid zygotes of unilateral crossing (WT × Pcp1-Ppc89-GFP). Using time-lapse microscopy, we observed the initial formation of a multipolar spindle that later transformed to a bipolar one and the eventual formation of four SPB clusters in the late stage of meiosis (Fig. 6 A). This is reminiscent of observations in cancer cells with extra centrosomes, in which multipolar spindle intermediates are formed initially and are resolved into bipolar spindles through centrosome clustering. This transition process enhances the formation of merotelic attachments and lagging chromosomes and thereby generates chromosome instability in cancer cells but avoids the complete failure of mitosis (Ganem et al., 2009; Nigg, 2002; Thompson and Compton, 2008). Studies have shown that spindle tension (traction forces onto spindle microtubules or tension on kinetochores) is required for centrosomal clustering. Reduced tension, for example, due to the destruction of chromatid cohesion or the disruption of microtubule–kinetochore attachment, leads to the formation of multipolar spindles because of reduced centrosomal clustering (Leber et al., 2010).

We speculated that spindle tension might also play a role in "SPB clustering" in fission yeast meiosis with extra SPBs. During polyploid meiosis, especially triploid meiosis, the presence of multiple homologues for each chromosome would result in unpaired homologues or polyvalent homologue pairing. These disordered pairings would compromise the generation of spindle tension, which might affect SPB clustering, thereby favoring the formation and stabilization of a multipolar spindle. In contrast, in diploids, proper homologue pairing would lead to proper kinetochore orientation and adequate spindle tension, which in turn promotes clustering of the extra SPBs and facilitates transforming a multipolar spindle to a bipolar one.

To test this reasoning, we abolished the spindle tension by disrupting homologue pairing in diploid meiosis. Deletion of *rec12*, whose protein product plays a conserved role in catalyzing the formation of double-strand DNA breaks to initiate homologous recombination in meiosis (Cervantes et al., 2000; Kan et al., 2011; Keeney et al., 1997), interferes with homologue pairing and prevents linkage between homologues (Cao et al., 1990; Cervantes et al., 2000). Therefore, in *rec12Δ* meiosis, spindle microtubules attach the chromosomes but lack tension because of unlinked homologues (Shonn et al., 2000). We observed that in diploid meiosis of a unilateral cross (Pcp1–Ppc89–GFP × WT) with *rec12* deletion, the percentage of asci containing extra spores increased compared with those carrying *rec12*^{wt}, despite the fact that the *rec12Δ* mutation alone compromised meiosis efficiency, causing a significant increase in the formation of asci containing fewer than four spores (Fig. 6 B). Deletion of *rec12* did not increase the percentage of extra spores in bilateral crosses of the fusion (Pcp1–Ppc89–GFP × Pcp1–Ppc89–GFP; Fig. 6 B), perhaps because the percentage of extra-spored asci was already high due to the more severe SPB quantity defect.

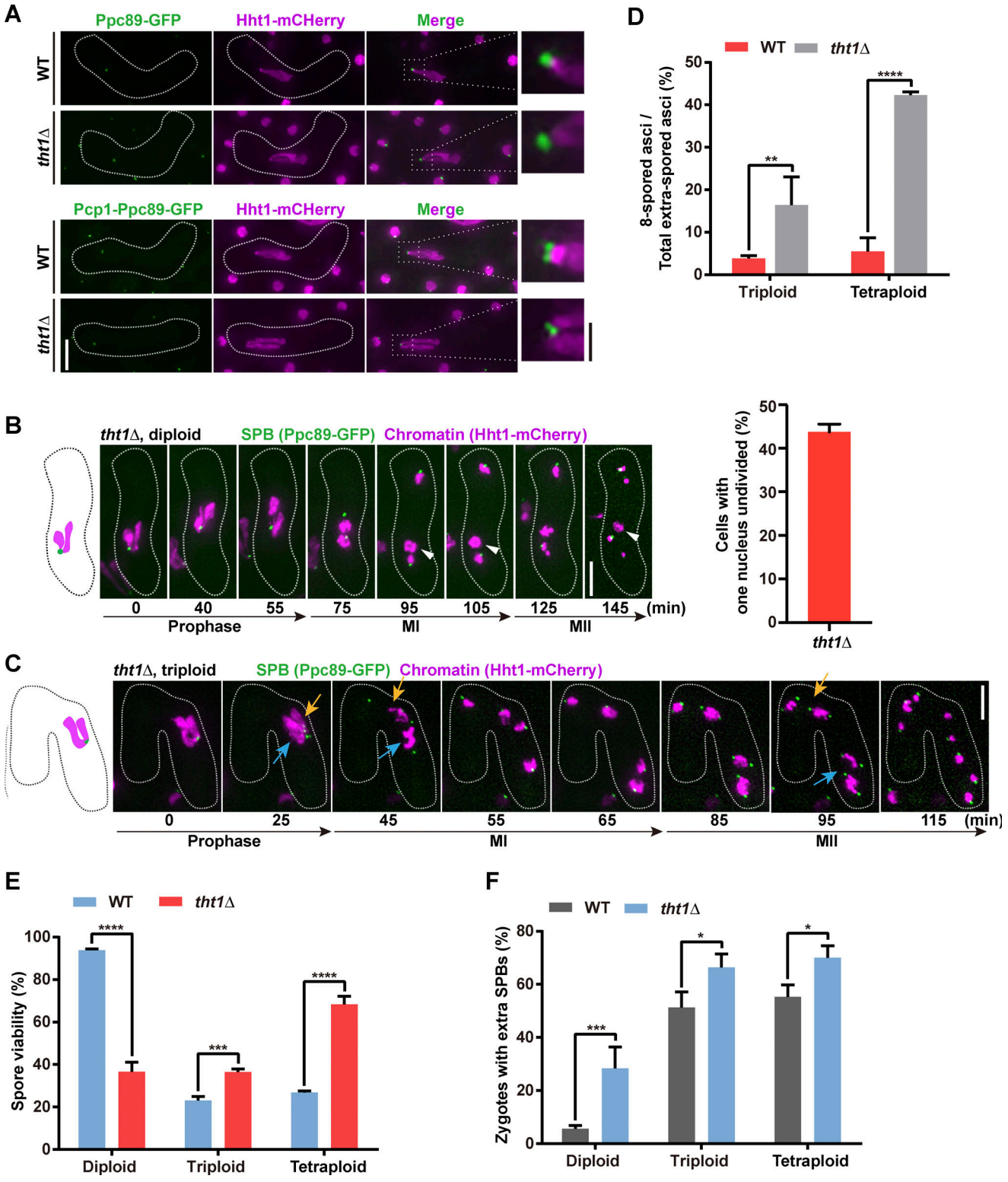

Figure 5. **Dissociation of Pcp1 from SPB is required for SPB fusion. (A)** Representative microscopic images of meiotic prophase in WT and *tht1Δ* zygotes expressing Ppc89-GFP (SPB) and Hht1-mCherry (chromatins; upper panels) or Pcp1–Ppc89–GFP (SPB) and Hht1-mCherry (chromatins; lower panels). Insets are enlargements of the boxed region. Scale bars: white, 5 µm; black, 1 µm. **(B and C)** Time-lapse images of *tht1Δ* diploid (B) or triploid (C) zygotes expressing Ppc89-GFP (SPB) and Hht1-mCherry (chromatins). Arrowheads indicate nuclei that are not involved in nuclear division in *tht1Δ* diploid zygotes. Arrows point to unfused nuclei undergoing meiosis separately in *tht1Δ* triploid zygotes. Time 0 is an arbitrary time point in horsetail stage. Scale bars, 5 µm. Quantification of cells with one nucleus not involved in nuclear division in *tht1Δ* diploid zygotes (B, right panels). Error bars are SDs from three independent experiments ($n \geq 100$ cells each). **(D)** Quantification of the proportion of asci containing eight spores in total extra-spored asci. $n \geq 150$ cells for each. **(E)** Quantification of spore viability from zygotic meiosis in the indicated ploidy and genetics background. **(F)** Quantification of zygotes with extra SPBs in the indicated ploidy and genetics background. $n \geq 200$ cells for each. Error bars in D–F are SDs from three independent experiments. *, $P < 0.05$; **, $P < 0.01$; ***, $P < 0.001$; ****, $P < 0.0001$ (two-way ANOVA with Šidák's multiple comparisons test).

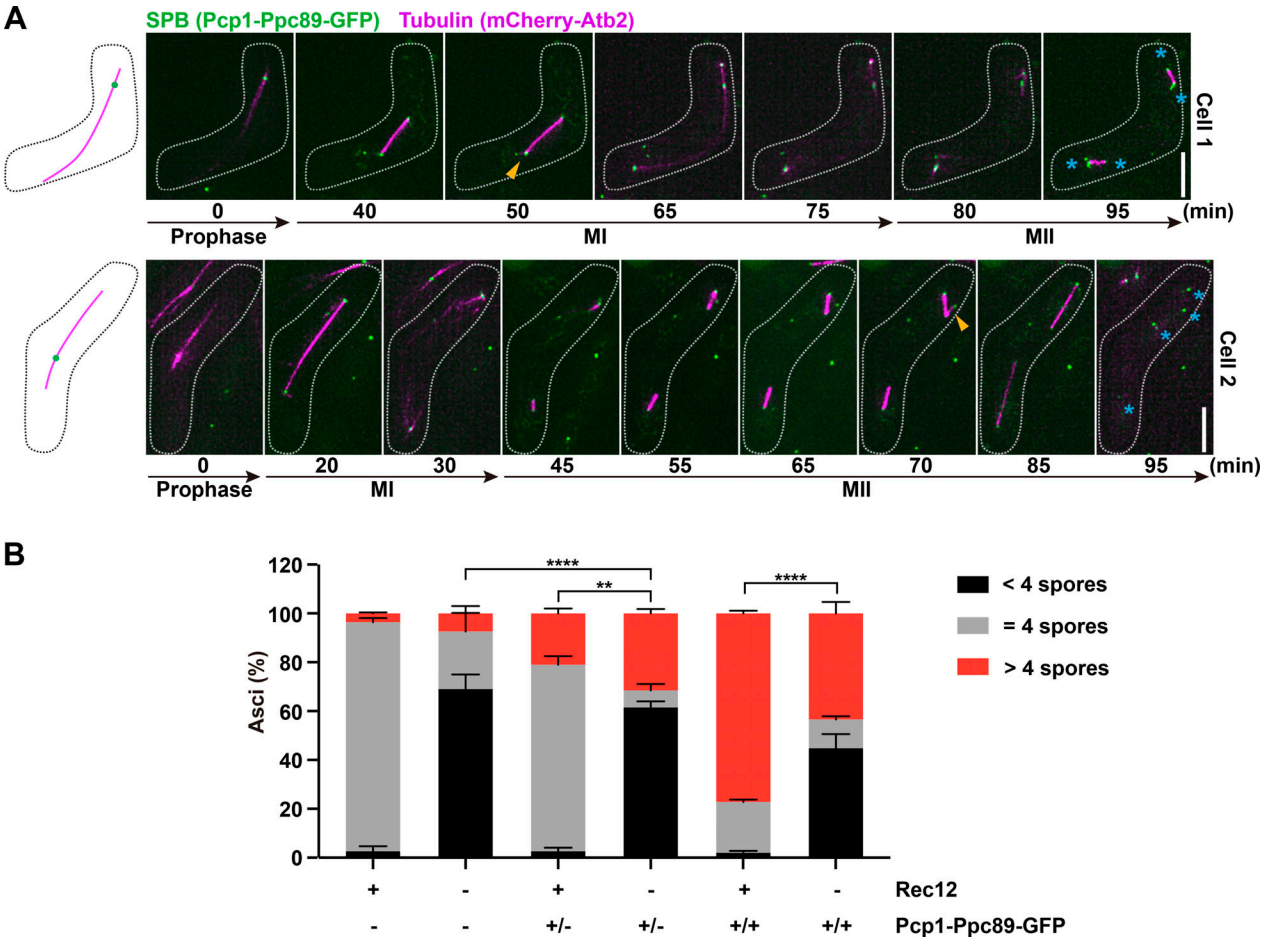

Figure 6. **Lack of homologue pairing enhances spindle multipolarity. (A)** Representative time-lapse images of diploid zygotes expressing Pcp1–Ppc89–GFP (SPB) and mCherry-Atb2 (microtubules). Arrowheads indicate multipolar spindle intermediates formed at MI and MII. Asterisks point to four clusters of SPBs formed at the late stage of meiosis. Time 0 is an arbitrary time point in prophase. Scale bars, 5 µm. **(B)** Quantification of zygotic asci with the indicated number of spores. +/−, unilateral cross of Pcp1–Ppc89–GFP; +/+, bilateral cross of Pcp1–Ppc89–GFP. Error bars are SDs from three independent experiments ($n \geq 200$ cells each). Asterisks indicate a significant difference for the greater-than-four spores category between the two samples being compared. **, $P < 0.01$; ****, $P < 0.0001$ (two-way ANOVA with Tukey's multiple comparisons test).

The results above suggest that SPB/centrosome clustering is a conserved process that can partially rescue the occurrence of harmful multipolar nuclear division in the presence of extra SPBs/centrosomes and that defective homologue pairing in polyploid meiosis inhibits this partial rescuing process.

Discussion

Dynamic regulation of Pcp1 localization is crucial for SPB homeostasis during sexual reproduction

A common proposition of sexually reproducing organisms is that the first cell (the zygote) inherits only one MTOC to support the first cell division. For metazoans, the realization of MTOC fusion requires the centrosomes of both gametes to undergo a "centrosome reduction" process before fusion (Schatten, 1994), whereas for unicellular yeast, our results show that temporary removal of Pcp1 from SPB is required for the fusion and the optimal quantity of SPBs in the zygote of *S. pombe* (Fig. 7). Ectopic tethering of Pcp1 to SPB is sufficient to block SPB fusion and results in extra SPBs in a diploid zygotic meiosis. This is reminiscent of "centrosome elimination" in *Drosophila melanogaster*, which requires the removal of PCM during ovum formation. A defect in centriole elimination caused by Polo-dependent PCM maintenance during ovum formation leads to abnormal meiosis of the eggs and aborted postfertilization embryo development (Pimenta-Marques et al., 2016). It is noteworthy that Pcp1 is an orthologue of pericentrin (a key component of PCM), and it has been shown that Polo kinase/Plo1 and Pcp1 have a complicated interaction relationship on the SPB (Ohta et al., 2012). Our work argues that this Pcp1-dependent process of alleviating surplus SPB ("SPB reduction") may be conserved in species ranging from yeast to metazoans for accurate SPB/centrosome inheritance during sexual reproduction.

How Pcp1 loses its dynamics on the SPB in polyploid zygotes is currently unknown. A simple model is that in polyploid zygotes, the larger SPB provided by the diploid mating partner possesses more anchor points for Pcp1 and therefore may take more time to accomplish the dislodging of Pcp1. In line with this idea, we consistently observed that in triploid meiosis, the haploid derived SPB successfully dislodges Pcp1, whereas the

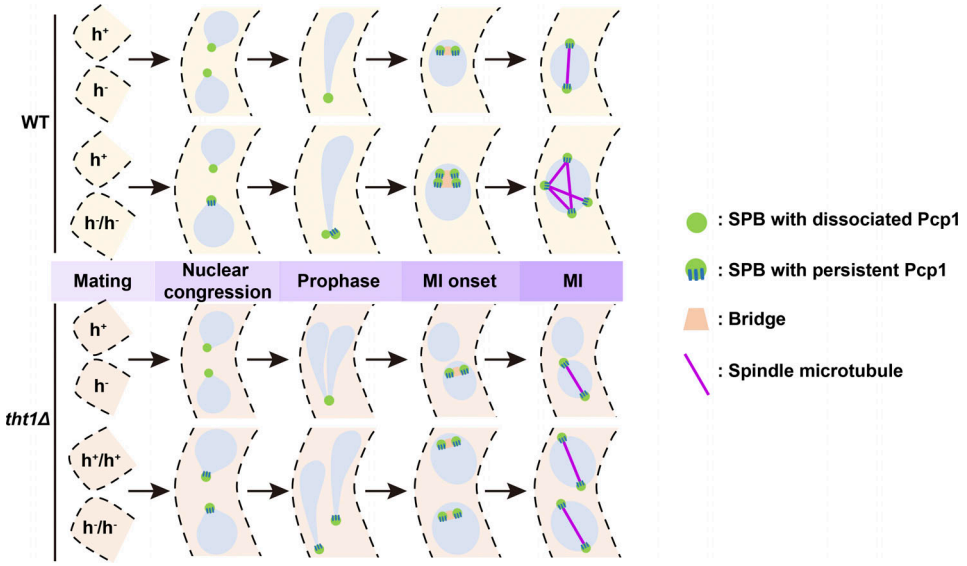

Figure 7. **A model for SPB quantity control in diploid and polyploid meiosis.** During zygotic meiosis of polyploids, the persistent localization of Pcp1 leads to the blockage of SPB fusion, resulting in the formation of supernumerary SPBs and multipolar nuclear division (upper panels). When the polyploid zygote also has a defect in NE fusion due to *tht1* deletion, twin meiosis will occur (lower panels).

diploid one does not, and, in our observation, there is no significant time delay in the process of polyploid meiosis compared with diploid meiosis.

In *S. cerevisiae*, SPB fusion also occurs, but its Pcp1 orthologue Spc110 has not been reported to have a sexual reproduction–specific dynamic association with the SPB (Lin et al., 2014). Moreover, although the viability of the spores produced by triploid meiosis in *S. cerevisiae* is also poor, there is no abnormality in the number of spores (Chen et al., 2020). An important difference between the SPB of these two yeasts is that, in *S. cerevisiae*, the SPB is embedded in the NE throughout the life cycle, whereas the SPB of *S. pombe* is located in the cytoplasm during interphase and inserted into the NE at the beginning of nuclear division (Cavanaugh and Jaspersen, 2017). This may lead to different SPB fusion mechanisms between these two yeasts because of the different local environments of the SPBs, as well as differences in the functional requirement on the SPB fusion for its quantity control. How Pcp1 plays a role in SPB fusion and its quantity control requires further investigation.

SPB/centrosome quantity control and ploidy evolution

The potential benefits of increased ploidy are multifold: for example, redundant genes can protect polyploids from deleterious mutations, and allopolyploids can acquire heterosis from hybridization (Comai, 2005). However, polyploidy is not adopted by most extant organisms, especially higher vertebrates. It seems that increased ploidy could have more deleterious impacts than potential benefits, although the deleterious impacts largely remain to be characterized in detail. Increased genome instability associated with increased ploidy may be a key constraint that limits the increase in ploidy. Single-celled yeasts are a desirable system for delineating the possible causal relationship between high ploidy and genome instability. Studies in budding yeast have shown that altered spindle geometry derived from the mismatches between SPB size, spindle length, and the size and geometry of the kinetochore is responsible for the genetic instability of tetraploids (Storchová et al., 2006). An increase in spindle assembly time, which scales linearly with chromosome number, is also linked with the genetic instability phenotype of polyploid *S. cerevisiae* cells (Jelenić et al., 2018).

Here, we show that in polyploid zygotes of *S. pombe*, blockage of SPB fusion results in extra SPBs that form multipolar spindles, which lead to abnormal chromosome segregation during subsequent meiosis or mitosis (if nutritional supply is restored; Fig. 7). Therefore, polyploid zygotes in which SPB fusion was blocked did not resume mitotic growth or maintain robust vegetative proliferation due to severe mitotic defects (Fig. S5 F). This may explain the previous unsuccessful attempts by others (Klinner and Böttcher, 1992; Molnar and Sipiczki, 1993) and us to generate stable polyploid *S. pombe* or *Pichia guilliermondii* strains by sexual hybridization. In contrast, for *S. cerevisiae*, polyploids up to hexaploidy can be readily constructed by hybridization (Querol and Bond, 2009). It seems that different yeasts have peculiarities in their cellular apparatus (most likely the cell division apparatus) and therefore have different abilities to tolerate and maintain polyploid genomes. Our present study suggests that the SPB is the key apparatus or is one of the key apparatuses in inhibiting polyploidy establishment in *S. pombe* due to the genetic instability caused by extra SPBs.

To our knowledge, this work is the first glimpse of the connection between ploidy and SPB quantity control in yeast. It is generally believed that, in tumors, extra centrosomes are acquired concomitantly with tetraploidization of the cells, but the mechanistic link between polyploidization and the formation of extra centrosomes is not fully understood (Baudoin et al., 2020; Ganem et al., 2009; Storchova and Pellman, 2004). Studies in mouse early embryos have shown that tetraploidization, even without initial concomitant doubling of centrosomes, leads to

the formation of extra centrosomes during subsequent cell division (Yaguchi et al., 2018), suggesting that polyploidization may play a dominant role in centrosome quantity dysregulation. This series of evidence suggests that the interaction between MTOC number dysregulation and polyploidy is conserved among organisms. Exploring this correlation in yeast may aid in understanding the relationship between extra centrosomes, polyploidization, and malignant behavior in cancers, which represents a major question in cancer biology, given that polyploidy and extra centrosomes alone are sufficient to drive tumorigenesis (Fujiwara et al., 2005; Levine et al., 2017). Finally, we propose that the strict restraint on the number of MTOCs may be a rate-limiting factor for ploidy increase in many organisms. Along this line, a correlation is noted in that higher plants form a centrosome-less spindle, and they have higher tolerance for polyploidy.

Abnormal homologue pairing and SPB quantity dysregulation play a combined role in polyploid meiosis

In the past, it was believed that the meiosis of polyploids, especially those with odd-numbered ploidy, are mainly influenced by defective homologue pairing and therefore are less likely to produce normal meiotic progeny. Here we demonstrate that an additional characteristic of polyploid meiosis in fission yeast is the frequent production of extra spores due to the SPB quantity dysregulation. Moreover, our data also indicate that the effects on meiosis due to homologue pairing defects and SPB number dysregulation are not independent. Rather, a lack of tension caused by abnormal homologue pairing may enhance the assembly of a multipolar spindle by suppressing SPB clustering.

An alternative and audacious possibility is that the increased number of SPBs in polyploids may serve as a way to compensate for the deficiency in homologue pairing, allowing multiple haploid spores to be produced through multipolar chromosome segregation and thus serving as a beneficiary meiotic mechanism to circumvent aneuploid formation in polyploid meiosis. Indeed, we have observed that a certain percentage of triploid zygotes can produce six viable haploid spores. Further investigation is required to verify this possibility.

Materials and methods

Strain construction and media

Strains of fission yeast used in this study are listed in Table S1. Standard molecular genetics techniques and media for *S. pombe* were used (Moreno et al., 1991). In general, standard PCR-based methods were used for GFP and mCherry tagging, gene deletion, and fusion protein construction (Bähler et al., 1998). To construct the strains with Pcp1–Ppc89–GFP or Cut12–Ppc89–GFP, *ppc89*$^{+}$ was cloned into the plasmid pYM27 before EGFP coding regions, then the resulting plasmid was used in the standard PCR-based gene-targeting procedures to tag the endogenous *pcp1*$^{+}$ or *cut12*$^{+}$ gene with Ppc89-GFP. To tether Plo1 to SPB, the expression vector pREP41 with the Plo1–Sid4C–GFP fusion construct was transformed into the corresponding strains. All transformants were verified by PCR. Primers used in this study are listed in Table S2. Strains with different fluorescent tags or mutations were obtained by standard crossing and tetrad dissection. Yeast cells were grown in yeast extract with essential supplements (YES) medium at 29°C unless indicated otherwise, and malt extract (ME) medium was used to induce mating and sporulation.

Diploid strains

The nonsporulating diploids were obtained from a DNA transformation process. Transformant colonies were preliminarily screened from colonies that were darkly stained on YES plates containing phloxin B. These diploids were then subjected to Hoechst staining followed by flow cytometry to verify their ploidy.

Flow cytometry

Freshly streaked cells were inoculated into liquid YES medium and incubated overnight at 29°C with 200-rpm shaking. The cell culture was refreshed the next morning and incubated at 29°C with 200-rpm shaking to exponential phase. Cells in exponential phase were fixed with 75% methanol and washed three times with YES medium. Then the cell samples were resuspended in PBS and stained with Hoechst 33342 DNA dye (5 µg/ml, H3570; Thermo Fisher Scientific) for 5 min at RT in the dark. The cell samples were washed three times with PBS and immediately analyzed on a Beckman CytoFLEX flow cytometer.

Fluorescence microscopy

Fluorescence microscopic images were acquired with a DeltaVision Elite microscope (Applied Precision) using a 60×/1.4 NA oil objective and a CoolSnap HQ2 camera (Photometrics). For time-lapse imaging, cells of opposite mating types were mixed on the ME agar plate to induce mating. After 6–8 h, a small aliquot of cell mixture was mounted onto a 2% agarose pad (in ME media) on a microscope slide covered with a coverslip. The agarose pad was set up in the DeltaVision Elite microscopy system, and the temperature was stably controlled at 29°C during imaging. For DNA staining, cells were fixed with 75% methanol and stained with 5 µg/ml Hoechst 33342 (H3570; Thermo Fisher Scientific). For all images, 10 or 20 Z-sections were collected, with the vertical distance between optical sections at 0.6 or 0.3 µm. Z-stacking images were deconvolved and combined into maximum intensity projections for analysis using SoftWorx (Applied Precision). Sporulated asci were photographed as brightfield or differential interference contrast images. Images were processed with Photoshop (Adobe) for publication.

EM

Cells induced to undergo meiosis on the ME plate were high-pressure frozen, freeze substituted, embedded, and stained for EM as described (Giddings et al., 2001). Briefly, after 7–8 h of nitrogen starvation, cells were harvested and then fixed by high-pressure freezing (Compact 01; Wohlwend Engineering). Cells were freeze substituted using the automatic freeze substitution system (Leica Microsystems) at −90°C in acetone containing 2% osmium tetroxide and 0.2% uranyl acetate and embedded in epon-Araldite. Serial sections (60 nm) were cut using an ultramicrotome (Leica EM UC7; Leica Microsystems). Sections were

collected on grids and post-stained with uranyl acetate and lead citrate. The sections were observed and imaged on a TECNAI spirit G2 transmission electron microscope (Thermo Fisher Scientific/FEI) operating at 120 kV.

Random spore assay

Cells were mated and sporulated on ME agar plates for 3 d at 29°C. The asci mixtures were taken off the plates and digested with Snailase for several hours at 30°C. Complete digestion of the ascus wall and gamete cells not involved in the mating was confirmed under the microscope. After counting, the spores were properly diluted and then spread on YES plates. The YES plates were incubated at 29°C for 3–4 d to allow countable colonies to form, and the number of colonies on each plate was counted. Spore viability was calculated as the number of colonies formed/number of spores spread.

Spotting assay

Serial dilution growth assays were performed by spotting 5 µl of yeast culture with an initial OD_{600} of 0.5–0.8 and its 5-fold or 10-fold serial dilutions on plates. The plates were incubated at 29°C for 3–4 d for growth assessment.

Statistical analysis

Data are presented as mean ± SD of three independent experiments. Student's *t* tests, one-way ANOVA tests, or two-way ANOVA tests were performed to determine the significance of the data as indicated in the figure legends. A P value <0.05 was considered statistically significant. Data distribution was assumed to be normal, but this was not formally tested. The number of cells counted and P values are described in the figure legends.

Online supplemental material

Fig. S1 shows that nonsporulating diploid strains undergo stable mitotic proliferation. Fig. S2 shows additional data for polyploid zygotic meiosis undergoing multipolar nuclear division. Fig. S3 shows additional data for the specific persistent localization of Pcp1 on the SPB in polyploid meiosis. Fig. S4 shows that cells with constitutive Pcp1–SPB association undergo normal mitotic proliferation and that zygotes with constitutive Cut12–SPB association have no abnormal SPB quantity regulation. Fig. S5 shows additional data indicating that the dissociation of Pcp1 from SPB is required for SPB fusion. Table S1 lists yeast strains used in this study. Table S2 lists primers used in this study.

Acknowledgments

We gratefully thank members of the He lab for helpful discussions and suggestions throughout the project and Takashi Toda (Hiroshima University, Hiroshima, Japan), Masayuki Yamamoto (University of Tokyo, Tokyo, Japan), and Masamitsu Sato (Waseda University, Tokyo, Japan) for kindly providing strains and plasmids. We thank the Center of Cryo-Electron Microscopy of Zhejiang University for technical support.

This work was supported by the National Natural Science Foundation of China (31671396 and 31871253 [to X. He]) and the Fundamental Research Funds for the Central Universities.

The authors declare no competing financial interests.

Author contributions: Q. Zhu and X. He conceived the project; Q. Zhu and X. He analyzed the data and wrote the manuscript; X. He directed the project; Q. Zhu constructed yeast strains and performed all experiments except the EM; Z. Jiang and Q. Zhu performed and analyzed EM; and X. He acquired funding.

Submitted: 22 April 2021
Revised: 31 August 2021
Accepted: 13 October 2021

References

Albertin, W., and P. Marullo. 2012. Polyploidy in fungi: evolution after whole-genome duplication. *Proc. Biol. Sci.* 279:2497–2509. https://doi.org/10.1098/rspb.2012.0434

Aoi, Y., K. Arai, M. Miyamoto, Y. Katsuta, A. Yamashita, M. Sato, and M. Yamamoto. 2013. Cuf2 boosts the transcription of APC/C activator Fzr1 to terminate the meiotic division cycle. *EMBO Rep.* 14:553–560. https://doi.org/10.1038/embor.2013.52

Bähler, J., J.Q. Wu, M.S. Longtine, N.G. Shah, A. McKenzie III, A.B. Steever, A. Wach, P. Philippsen, and J.R. Pringle. 1998. Heterologous modules for efficient and versatile PCR-based gene targeting in *Schizosaccharomyces pombe*. *Yeast*. 14:943–951. https://doi.org/10.1002/(SICI)1097-0061(199807)14:10<943::AID-YEA292>3.0.CO;2-Y

Basto, R., K. Brunk, T. Vinadogrova, N. Peel, A. Franz, A. Khodjakov, and J.W. Raff. 2008. Centrosome amplification can initiate tumorigenesis in flies. *Cell.* 133:1032–1042. https://doi.org/10.1016/j.cell.2008.05.039

Baudoin, N.C., J.M. Nicholson, K. Soto, O. Martin, J. Chen, and D. Cimini. 2020. Asymmetric clustering of centrosomes defines the early evolution of tetraploid cells. *eLife.* 9:e54565. https://doi.org/10.7554/eLife.54565

Bestul, A.J., Z. Yu, J.R. Unruh, and S.L. Jaspersen. 2017. Molecular model of fission yeast centrosome assembly determined by superresolution imaging. *J. Cell Biol.* 216:2409–2424. https://doi.org/10.1083/jcb.201701041

Bettencourt-Dias, M., and D.M. Glover. 2007. Centrosome biogenesis and function: centrosomics brings new understanding. *Nat. Rev. Mol. Cell Biol.* 8:451–463. https://doi.org/10.1038/nrm2180

Cao, L., E. Alani, and N. Kleckner. 1990. A pathway for generation and processing of double-strand breaks during meiotic recombination in *S. cerevisiae*. *Cell.* 61:1089–1101. https://doi.org/10.1016/0092-8674(90)90072-M

Cavanaugh, A.M., and S.L. Jaspersen. 2017. Big lessons from little yeast: budding and fission yeast centrosome structure, duplication, and function. *Annu. Rev. Genet.* 51:361–383. https://doi.org/10.1146/annurev-genet-120116-024733

Cervantes, M.D., J.A. Farah, and G.R. Smith. 2000. Meiotic DNA breaks associated with recombination in *S. pombe*. *Mol. Cell.* 5:883–888. https://doi.org/10.1016/S1097-2765(00)80328-7

Chen, J., Z. Xiong, D.E. Miller, Z. Yu, S. McCroskey, W.D. Bradford, A.M. Cavanaugh, and S.L. Jaspersen. 2020. The role of gene dosage in budding yeast centrosome scaling and spontaneous diploidization. *PLoS Genet.* 16:e1008911. https://doi.org/10.1371/journal.pgen.1008911

Comai, L. 2005. The advantages and disadvantages of being polyploid. *Nat. Rev. Genet.* 6:836–846. https://doi.org/10.1038/nrg1711

Ding, D.Q., Y. Chikashige, T. Haraguchi, and Y. Hiraoka. 1998. Oscillatory nuclear movement in fission yeast meiotic prophase is driven by astral microtubules, as revealed by continuous observation of chromosomes and microtubules in living cells. *J. Cell Sci.* 111:701–712. https://doi.org/10.1242/jcs.111.6.701

Edgar, B.A., and T.L. Orr-Weaver. 2001. Endoreplication cell cycles: more for less. *Cell.* 105:297–306. https://doi.org/10.1016/S0092-8674(01)00334-8

Egel, R., and M. Egel-Mitani. 1974. Premeiotic DNA synthesis in fission yeast. *Exp. Cell Res.* 88:127–134. https://doi.org/10.1016/0014-4827(74)90626-0

Flory, M.R., M. Morphew, J.D. Joseph, A.R. Means, and T.N. Davis. 2002. Pcp1p, an Spc110p-related calmodulin target at the centrosome of the fission yeast *Schizosaccharomyces pombe*. *Cell Growth Differ.* 13:47–58.

Fong, C.S., M. Sato, and T. Toda. 2010. Fission yeast Pcp1 links polo kinase-mediated mitotic entry to γ-tubulin-dependent spindle formation. *EMBO J.* 29:120–130. https://doi.org/10.1038/emboj.2009.331

Fujiwara, T., M. Bandi, M. Nitta, E.V. Ivanova, R.T. Bronson, and D. Pellman. 2005. Cytokinesis failure generating tetraploids promotes tumorigenesis in p53-null cells. *Nature.* 437:1043–1047. https://doi.org/10.1038/nature04217

Ganem, N.J., S.A. Godinho, and D. Pellman. 2009. A mechanism linking extra centrosomes to chromosomal instability. *Nature.* 460:278–282. https://doi.org/10.1038/nature08136

Giddings, T.H. Jr., E.T. O'Toole, M. Morphew, D.N. Mastronarde, J.R. McIntosh, and M. Winey. 2001. Using rapid freeze and freeze-substitution for the preparation of yeast cells for electron microscopy and three-dimensional analysis. *Methods Cell Biol.* 67:27–42. https://doi.org/10.1016/S0091-679X(01)67003-1

Grandont, L., E. Jenczewski, and A. Lloyd. 2013. Meiosis and its deviations in polyploid plants. *Cytogenet. Genome Res.* 140:171–184. https://doi.org/10.1159/000351730

Gutz, H. 1967. "Twin meiosis" and other ambivalences in the life cycle of *Schizosaccharomyces pombe*. *Science.* 158:796–798. https://doi.org/10.1126/science.158.3802.796

Hagan, I., and M. Yanagida. 1995. The product of the spindle formation gene sad1+ associates with the fission yeast spindle pole body and is essential for viability. *J. Cell Biol.* 129:1033–1047. https://doi.org/10.1083/jcb.129.4.1033

Harari, Y., Y. Ram, N. Rappoport, L. Hadany, and M. Kupiec. 2018. Spontaneous changes in ploidy are common in yeast. *Curr. Biol.* 28:825–835.e4. https://doi.org/10.1016/j.cub.2018.01.062

Ito, D., S. Zitouni, S.C. Jana, P. Duarte, J. Surkont, Z. Carvalho-Santos, J.B. Pereira-Leal, M.G. Ferreira, and M. Bettencourt-Dias. 2019. Pericentrin-mediated SAS-6 recruitment promotes centriole assembly. *eLife.* 8:e41418. https://doi.org/10.7554/eLife.41418

Jelenić, I., A. Selmecki, L. Laan, and N. Pavin. 2018. Spindle dynamics model explains chromosome loss rates in yeast polyploid cells. *Front. Genet.* 9:296. https://doi.org/10.3389/fgene.2018.00296

Jin, Y., J.J. Mancuso, S. Uzawa, D. Cronembold, and W.Z. Cande. 2005. The fission yeast homolog of the human transcription factor EAP30 blocks meiotic spindle pole body amplification. *Dev. Cell.* 9:63–73. https://doi.org/10.1016/j.devcel.2005.04.016

Kan, F., M.K. Davidson, and W.P. Wahls. 2011. Meiotic recombination protein Rec12: functional conservation, crossover homeostasis and early crossover/non-crossover decision. *Nucleic Acids Res.* 39:1460–1472. https://doi.org/10.1093/nar/gkq993

Keeney, S., C.N. Giroux, and N. Kleckner. 1997. Meiosis-specific DNA double-strand breaks are catalyzed by Spo11, a member of a widely conserved protein family. *Cell.* 88:375–384. https://doi.org/10.1016/S0092-8674(00)81876-0

Kilmartin, J.V. 2003. Sfi1p has conserved centrin-binding sites and an essential function in budding yeast spindle pole body duplication. *J. Cell Biol.* 162:1211–1221. https://doi.org/10.1083/jcb.200307064

Kilmartin, J.V. 2014. Lessons from yeast: the spindle pole body and the centrosome. *Philos. Trans. R. Soc. Lond. B Biol. Sci.* 369:20130456. https://doi.org/10.1098/rstb.2013.0456

Klinner, U., and F. Böttcher. 1992. Mitotically unstable polyploids in the yeast *Pichia guilliermondii*. *J. Basic Microbiol.* 32:331–338. https://doi.org/10.1002/jobm.3620320509

Krapp, A., E.C. Del Rosario, and V. Simanis. 2010. The role of *Schizosaccharomyces pombe* dma1 in spore formation during meiosis. *J. Cell Sci.* 123:3284–3293. https://doi.org/10.1242/jcs.069112

Kurihara, L.J., C.T. Beh, M. Latterich, R. Schekman, and M.D. Rose. 1994. Nuclear congression and membrane fusion: two distinct events in the yeast karyogamy pathway. *J. Cell Biol.* 126:911–923. https://doi.org/10.1083/jcb.126.4.911

Leber, B., B. Maier, F. Fuchs, J. Chi, P. Riffel, S. Anderhub, L. Wagner, A.D. Ho, J.L. Salisbury, M. Boutros, et al. 2010. Proteins required for centrosome clustering in cancer cells. *Sci. Transl. Med.* 2:33ra38. https://doi.org/10.1126/scitranslmed.3000915

Lee, I.J., N. Wang, W. Hu, K. Schott, J. Bähler, T.H. Giddings Jr., J.R. Pringle, L.L. Du, and J.Q. Wu. 2014. Regulation of spindle pole body assembly and cytokinesis by the centrin-binding protein Sfi1 in fission yeast. *Mol. Biol. Cell.* 25:2735–2749. https://doi.org/10.1091/mbc.e13-11-0699

Levine, M.S., B. Bakker, B. Boeckx, J. Moyett, J. Lu, B. Vitre, D.C. Spierings, P.M. Lansdorp, D.W. Cleveland, D. Lambrechts, et al. 2017. Centrosome amplification is sufficient to promote spontaneous tumorigenesis in mammals. *Dev. Cell.* 40:313–322.e5. https://doi.org/10.1016/j.devcel.2016.12.022

Lin, T.C., A. Neuner, Y.T. Schlosser, A.N. Scharf, L. Weber, and E. Schiebel. 2014. Cell-cycle dependent phosphorylation of yeast pericentrin regulates γ-TuSC-mediated microtubule nucleation. *eLife.* 3:e02208. https://doi.org/10.7554/eLife.02208

Lin, T.C., A. Neuner, and E. Schiebel. 2015. Targeting of γ-tubulin complexes to microtubule organizing centers: conservation and divergence. *Trends Cell Biol.* 25:296–307. https://doi.org/10.1016/j.tcb.2014.12.002

Lingle, W.L., W.H. Lutz, J.N. Ingle, N.J. Maihle, and J.L. Salisbury. 1998. Centrosome hypertrophy in human breast tumors: implications for genomic stability and cell polarity. *Proc. Natl. Acad. Sci. USA.* 95:2950–2955. https://doi.org/10.1073/pnas.95.6.2950

Loncarek, J., P. Hergert, V. Magidson, and A. Khodjakov. 2008. Control of daughter centriole formation by the pericentriolar material. *Nat. Cell Biol.* 10:322–328. https://doi.org/10.1038/ncb1694

Manandhar, G., H. Schatten, and P. Sutovsky. 2005. Centrosome reduction during gametogenesis and its significance. *Biol. Reprod.* 72:2–13. https://doi.org/10.1095/biolreprod.104.031245

Mayer, V.W., and A. Aguilera. 1990. High levels of chromosome instability in polyploids of *Saccharomyces cerevisiae*. *Mutat. Res.* 231:177–186. https://doi.org/10.1016/0027-5107(90)90024-X

Melloy, P., S. Shen, E. White, J.R. McIntosh, and M.D. Rose. 2007. Nuclear fusion during yeast mating occurs by a three-step pathway. *J. Cell Biol.* 179:659–670. https://doi.org/10.1083/jcb.200706151

Mikeladze-Dvali, T., L. von Tobel, P. Strnad, G. Knott, H. Leonhardt, L. Schermelleh, and P. Gönczy. 2012. Analysis of centriole elimination during *C. elegans* oogenesis. *Development.* 139:1670–1679. https://doi.org/10.1242/dev.075440

Molnar, M., and M. Sipiczki. 1993. Polyploidy in the haplontic yeast *Schizosaccharomyces pombe*: construction and analysis of strains. *Curr. Genet.* 24:45–52. https://doi.org/10.1007/BF00324664

Moreno, S., A. Klar, and P. Nurse. 1991. Molecular genetic analysis of fission yeast *Schizosaccharomyces pombe*. *Methods Enzymol.* 194:795–823. https://doi.org/10.1016/0076-6879(91)94059-L

Nigg, E.A. 2002. Centrosome aberrations: cause or consequence of cancer progression? *Nat. Rev. Cancer.* 2:815–825. https://doi.org/10.1038/nrc924

Nishikawa, S., A. Hirata, and T. Endo. 2008. Nuclear inner membrane fusion facilitated by yeast Jem1p is required for spindle pole body fusion but not for the first mitotic nuclear division during yeast mating. *Genes Cells.* 13:1185–1195. https://doi.org/10.1111/j.1365-2443.2008.01236.x

Niwa, O., and M. Yanagida. 1985. Triploid meiosis and aneuploidy in *Schizosaccharomyces pombe*: an unstable aneuploid disomic for chromosome III. *Curr. Genet.* 9:463–470. https://doi.org/10.1007/BF00434051

Ohta, M., M. Sato, and M. Yamamoto. 2012. Spindle pole body components are reorganized during fission yeast meiosis. *Mol. Biol. Cell.* 23:1799–1811. https://doi.org/10.1091/mbc.e11-11-0951

Otto, S.P. 2007. The evolutionary consequences of polyploidy. *Cell.* 131:452–462. https://doi.org/10.1016/j.cell.2007.10.022

Otto, S.P., and J. Whitton. 2000. Polyploid incidence and evolution. *Annu. Rev. Genet.* 34:401–437. https://doi.org/10.1146/annurev.genet.34.1.401

Pihan, G.A., A. Purohit, J. Wallace, R. Malhotra, L. Liotta, and S.J. Doxsey. 2001. Centrosome defects can account for cellular and genetic changes that characterize prostate cancer progression. *Cancer Res.* 61:2212–2219.

Pimenta-Marques, A., I. Bento, C.A. Lopes, P. Duarte, S.C. Jana, and M. Bettencourt-Dias. 2016. A mechanism for the elimination of the female gamete centrosome in *Drosophila melanogaster*. *Science.* 353:aaf4866. https://doi.org/10.1126/science.aaf4866

Polakova, S., Z. Benko, L. Zhang, and J. Gregan. 2014. Mal3, the *Schizosaccharomyces pombe* homolog of EB1, is required for karyogamy and for promoting oscillatory nuclear movement during meiosis. *Cell Cycle.* 13:72–77. https://doi.org/10.4161/cc.26815

Querol, A., and U. Bond. 2009. The complex and dynamic genomes of industrial yeasts. *FEMS Microbiol. Lett.* 293:1–10. https://doi.org/10.1111/j.1574-6968.2008.01480.x

Rüthnick, D., and E. Schiebel. 2016. Duplication of the yeast spindle pole body once per cell cycle. *Mol. Cell. Biol.* 36:1324–1331. https://doi.org/10.1128/MCB.00048-16

Saito, T.T., T. Tougan, D. Okuzaki, T. Kasama, and H. Nojima. 2005. Mcp6, a meiosis-specific coiled-coil protein of *Schizosaccharomyces pombe*, localizes to the spindle pole body and is required for horsetail movement and recombination. *J. Cell Sci.* 118:447–459. https://doi.org/10.1242/jcs.01629

Sakuno, T., K. Tada, and Y. Watanabe. 2009. Kinetochore geometry defined by cohesion within the centromere. *Nature.* 458:852–858. https://doi.org/10.1038/nature07876

Sakuno, T., K. Tanaka, S. Hauf, and Y. Watanabe. 2011. Repositioning of aurora B promoted by chiasmata ensures sister chromatid mono-orientation

in meiosis I. *Dev. Cell.* 21:534–545. https://doi.org/10.1016/j.devcel.2011.08.012

Schatten, G. 1994. The centrosome and its mode of inheritance: the reduction of the centrosome during gametogenesis and its restoration during fertilization. *Dev. Biol.* 165:299–335. https://doi.org/10.1006/dbio.1994.1256

Shonn, M.A., R. McCarroll, and A.W. Murray. 2000. Requirement of the spindle checkpoint for proper chromosome segregation in budding yeast meiosis. *Science.* 289:300–303. https://doi.org/10.1126/science.289.5477.300

Sipiczki, M. 1988. The role of sterility genes (ste and aff) in the initiation of sexual development in *Schizosaccharomyces pombe*. *Mol. Gen. Genet.* 213:529–534. https://doi.org/10.1007/BF00339626

Sipiczki, M., and L. Ferenczy. 1977. Protoplast fusion of *Schizosaccharomyces pombe* auxotrophic mutants of identical mating-type. *Mol. Gen. Genet.* 151:77–81. https://doi.org/10.1007/BF00446915

St. Charles, J., M.L. Hamilton, and T.D. Petes. 2010. Meiotic chromosome segregation in triploid strains of *Saccharomyces cerevisiae*. *Genetics.* 186:537–550. https://doi.org/10.1534/genetics.110.121533

Storchova, Z., and D. Pellman. 2004. From polyploidy to aneuploidy, genome instability and cancer. *Nat. Rev. Mol. Cell Biol.* 5:45–54. https://doi.org/10.1038/nrm1276

Storchová, Z., A. Breneman, J. Cande, J. Dunn, K. Burbank, E. O'Toole, and D. Pellman. 2006. Genome-wide genetic analysis of polyploidy in yeast. *Nature.* 443:541–547. https://doi.org/10.1038/nature05178

Tanaka, K., and A. Hirata. 1982. Ascospore development in the fission yeasts *Schizosaccharomyces pombe* and *S. japonicus*. *J. Cell Sci.* 56:263–279. https://doi.org/10.1242/jcs.56.1.263

Tanaka, K., T. Kohda, A. Yamashita, N. Nonaka, and M. Yamamoto. 2005. Hrs1p/Mcp6p on the meiotic SPB organizes astral microtubule arrays for oscillatory nuclear movement. *Curr. Biol.* 15:1479–1486. https://doi.org/10.1016/j.cub.2005.07.058

Tang, N.H., N. Okada, C.S. Fong, K. Arai, M. Sato, and T. Toda. 2014. Targeting Alp7/TACC to the spindle pole body is essential for mitotic spindle assembly in fission yeast. *FEBS Lett.* 588:2814–2821. https://doi.org/10.1016/j.febslet.2014.06.027

Tang, N.H., C.S. Fong, H. Masuda, I. Jourdain, M. Yukawa, and T. Toda. 2019. Generation of temperature sensitive mutations with error-prone PCR in a gene encoding a component of the spindle pole body in fission yeast. *Biosci. Biotechnol. Biochem.* 83:1717–1720. https://doi.org/10.1080/09168451.2019.1611414

Tange, Y., T. Horio, M. Shimanuki, D.Q. Ding, Y. Hiraoka, and O. Niwa. 1998. A novel fission yeast gene, tht1+, is required for the fusion of nuclear envelopes during karyogamy. *J. Cell Biol.* 140:247–258. https://doi.org/10.1083/jcb.140.2.247

Tel-Zur, N., S. Abbo, and Y. Mizrahi. 2005. Cytogenetics of semi-fertile triploid and aneuploid intergeneric vine cacti hybrids. *J. Hered.* 96:124–131. https://doi.org/10.1093/jhered/esi012

Thompson, S.L., and D.A. Compton. 2008. Examining the link between chromosomal instability and aneuploidy in human cells. *J. Cell Biol.* 180:665–672. https://doi.org/10.1083/jcb.200712029

Wang, F., R. Zhang, W. Feng, D. Tsuchiya, O. Ballew, J. Li, V. Denic, and S. Lacefield. 2020. Autophagy of an amyloid-like translational repressor regulates meiotic exit. *Dev. Cell.* 52:141–151.e5. https://doi.org/10.1016/j.devcel.2019.12.017

Widra, A., and E.D. De Lamater. 1954. Cytologic studies of meiosis in *Schizosaccharomyces octosporus*. *Trans. N. Y. Acad. Sci.* 16(7 Series II):370. https://doi.org/10.1111/j.2164-0947.1954.tb01179.x

Wolfe, K.H., and D.C. Shields. 1997. Molecular evidence for an ancient duplication of the entire yeast genome. *Nature.* 387:708–713. https://doi.org/10.1038/42711

Yaguchi, K., T. Yamamoto, R. Matsui, M. Shimada, A. Shibanuma, K. Kamimura, T. Koda, and R. Uehara. 2018. Tetraploidy-associated centrosome overduplication in mouse early embryos. *Commun. Integr. Biol.* 11:e1526605. https://doi.org/10.1080/19420889.2018.1526605

Supplemental material

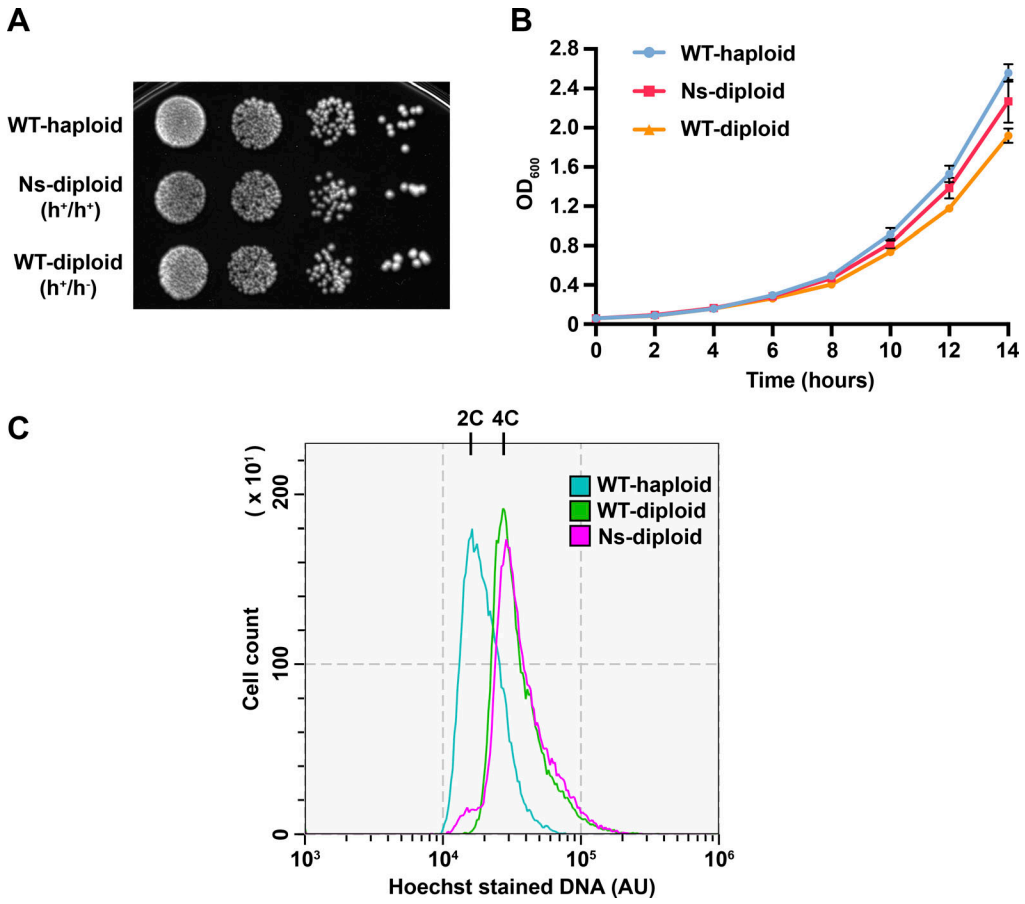

Figure S1. **Nonsporulating diploid strains undergo stable mitotic proliferation. (A)** Serial dilution growth assays for each indicated strain. **(B)** Growth curves of WT-haploid, Ns-diploid, and WT-diploid cells in YES medium at 29°C. Error bars show mean ± SD of the results of three independent experiments. **(C)** Flow cytometric analysis of DNA in cells of corresponding ploidy (n = 30,000). 2C, haploid DNA content; 4C, diploid DNA content; Ns-diploid, non-sporulating diploid.

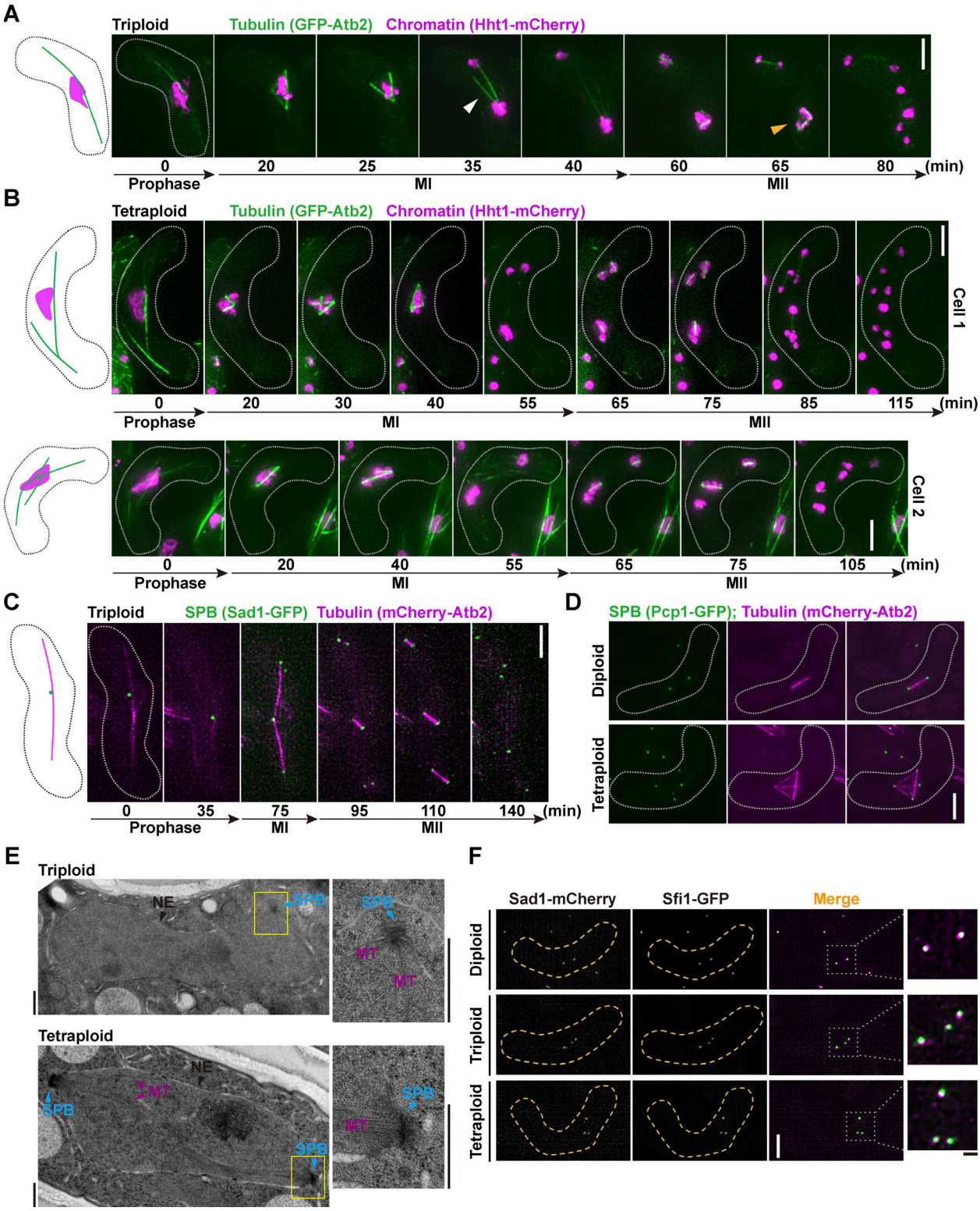

Figure S2. **Multipolar nuclear division occurs in polyploid zygotic meiosis. (A)** Representative time-lapse images of triploid zygotes expressing GFP-Atb2 (microtubules) and Hht1-mCherry (chromatins). White arrowhead points to uneven nuclear division at MI, and yellow arrowhead points to a multipolar spindle at MII. **(B)** Representative time-lapse images of tetraploid zygotes expressing GFP-Atb2 (microtubules) and Hht1-mCherry (chromatins). **(C)** Representative time-lapse images of triploid zygotes expressing Sad1-GFP (SPB) and mCherry-Atb2 (microtubules). Time 0 is an arbitrary time point in meiotic prophase. **(D)** Representative microscopic images of MI in diploid and tetraploid zygotes expressing Pcp1-GFP (SPB) and mCherry-Atb2 (microtubules). **(E)** Transmission electron micrographs of MI nuclei in triploid and tetraploid zygotes. The boxed regions are magnified to the right. Scale bars, 500 nm. MT, microtubule. **(F)** Microscopic images of MI in zygotes with different ploidy expressing Sad1-mCherry and Sfi1-GFP (half-bridge). Insets are enlargements of the boxed region. Scale bars: white, 5 µm; black, 1 µm. Scale bars in A–D, 5 µm.

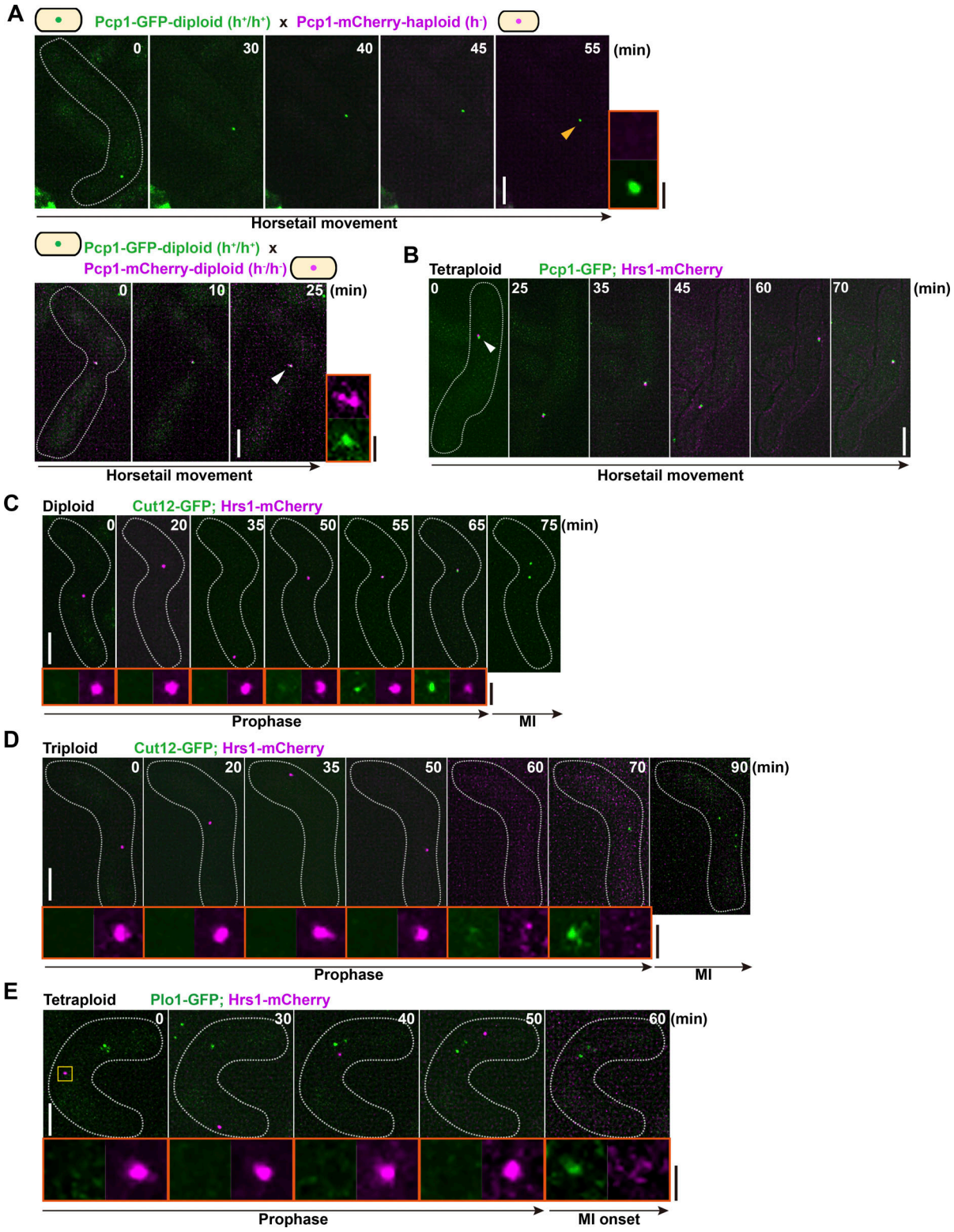

Figure S3. **The dynamics of Cut12 and Plo1 on the SPB is maintained in polyploid zygotes. (A)** Representative time-lapse images of zygotes from mating between two gametes with indicated ploidy expressing Pcp1-GFP and Pcp1-mCherry, respectively. Yellow arrowhead points to SPB with only Pcp1-GFP persisting on it in the triploid zygote, and white arrowhead points to SPB with Pcp1-GFP and Pcp1-mCherry persisting on it in the tetraploid zygote. SPBs indicated by arrowheads are enlarged in insets. Diagrams show the mating partners. **(B)** Representative time-lapse images of tetraploid zygotes expressing Pcp1-GFP and Hrs1-mCherry. Arrowhead points to Pcp1-GFP dot persisting on the SPB throughout prophase. Scale bar, 5 µm. **(C and D)** Time-lapse images of diploid (C) or triploid (D) zygotes expressing Cut12-GFP and Hrs1-mCherry. Insets are enlargements of the corresponding SPB dots. **(E)** Representative time-lapse images of meiotic prophase in tetraploid zygotes expressing Plo1-GFP and Hrs1-mCherry. Insets are enlargements of the corresponding SPB dots. Time 0 in A, C, D, and E is an arbitrary time point in early prophase. Scale bars: white, 5 µm; black, 1 µm.

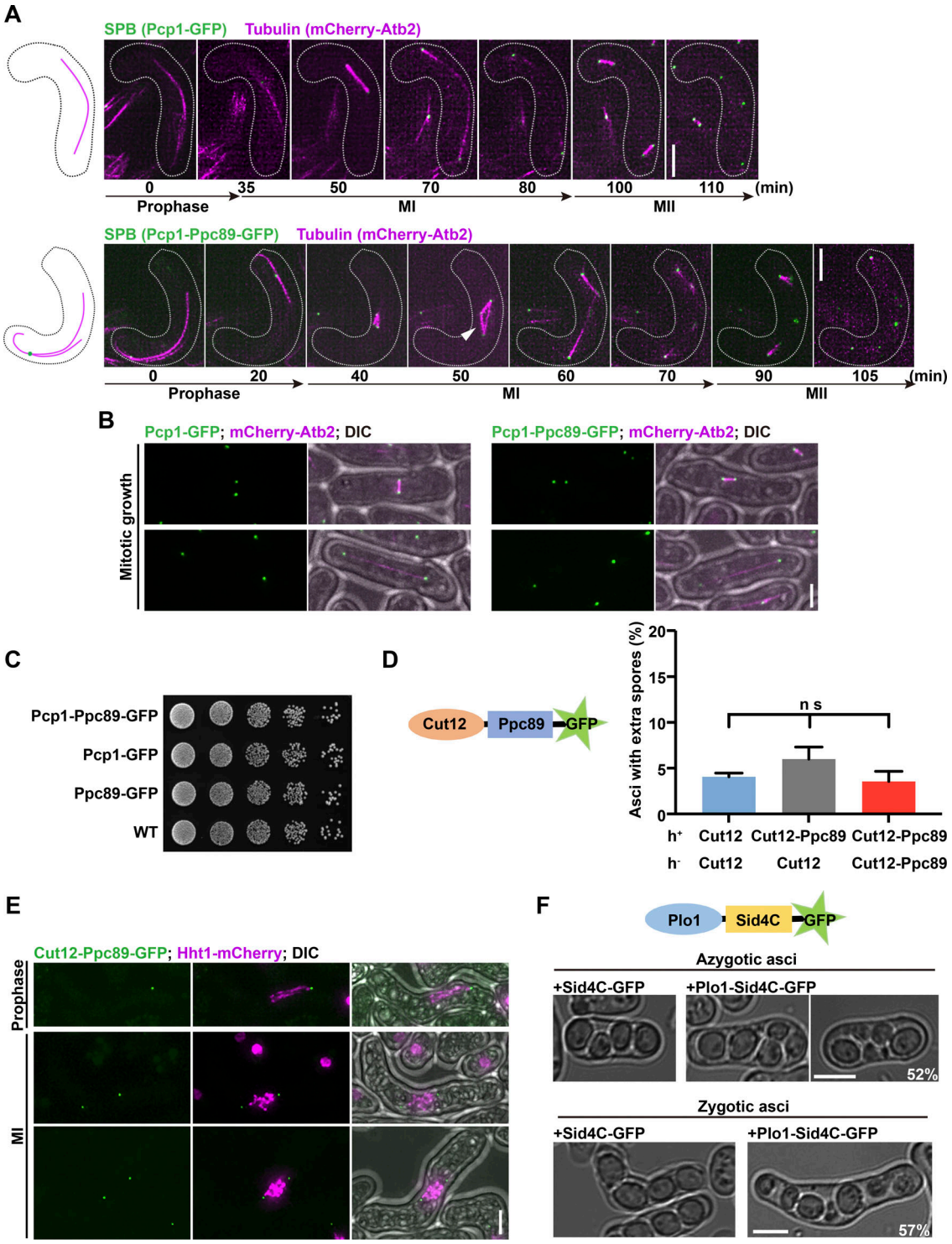

Figure S4. **Cells expressing Pcp1–Ppc89–GFP undergo normal mitotic growth, and forced Cut12–SPB association has no effect on SPB quantity control. (A)** Representative time-lapse images of zygotes expressing Pcp1-GFP (SPB) and mCherry-Atb2 (microtubules; upper panels) or Pcp1–Ppc89–GFP (SPB) and mCherry-Atb2 (microtubules; lower panels). Arrowhead indicates a multipolar spindle with supernumerary SPBs formed at MI. Time 0 is an arbitrary time point in prophase. Scale bars, 5 µm. **(B)** Microscopic images of mitosis in cells expressing Pcp1-GFP (SPB) and mCherry-Atb2 (microtubules; left panels) or Pcp1–Ppc89–GFP (SPB) and mCherry-Atb2 (microtubules; right panels). Scale bar, 3 µm. **(C)** Serial dilution growth assays for each indicated strain. **(D)** Schematic of Cut12–Ppc89–GFP construct used to force association between Cut12 and SPB (left). Quantification of asci containing extra spores in the indicated crosses (right). Cut12, Cut12-GFP; Cut12-Ppc89, Cut12–Ppc89–GFP. Error bars are SDs from three independent experiments ($n \geq 200$ cells each; one-way ANOVA). **(E)** Representative microscopic images of prophase and MI in zygotes expressing Cut12–Ppc89–GFP (SPB) and Hht1-mCherry (chromatins). Scale bar, 5 µm. **(F)** Representative microscopic images of azygotic and zygotic asci expressing Plo1–Sid4C–GFP or Sid4C-GFP. Plo1–Sid4C–GFP fusion construct is used to tether Plo1 to SPB during meiotic prophase. Percentages of asci with extra spores are shown in the lower right. Scale bar, 5 µm. DIC, differential interference contrast.

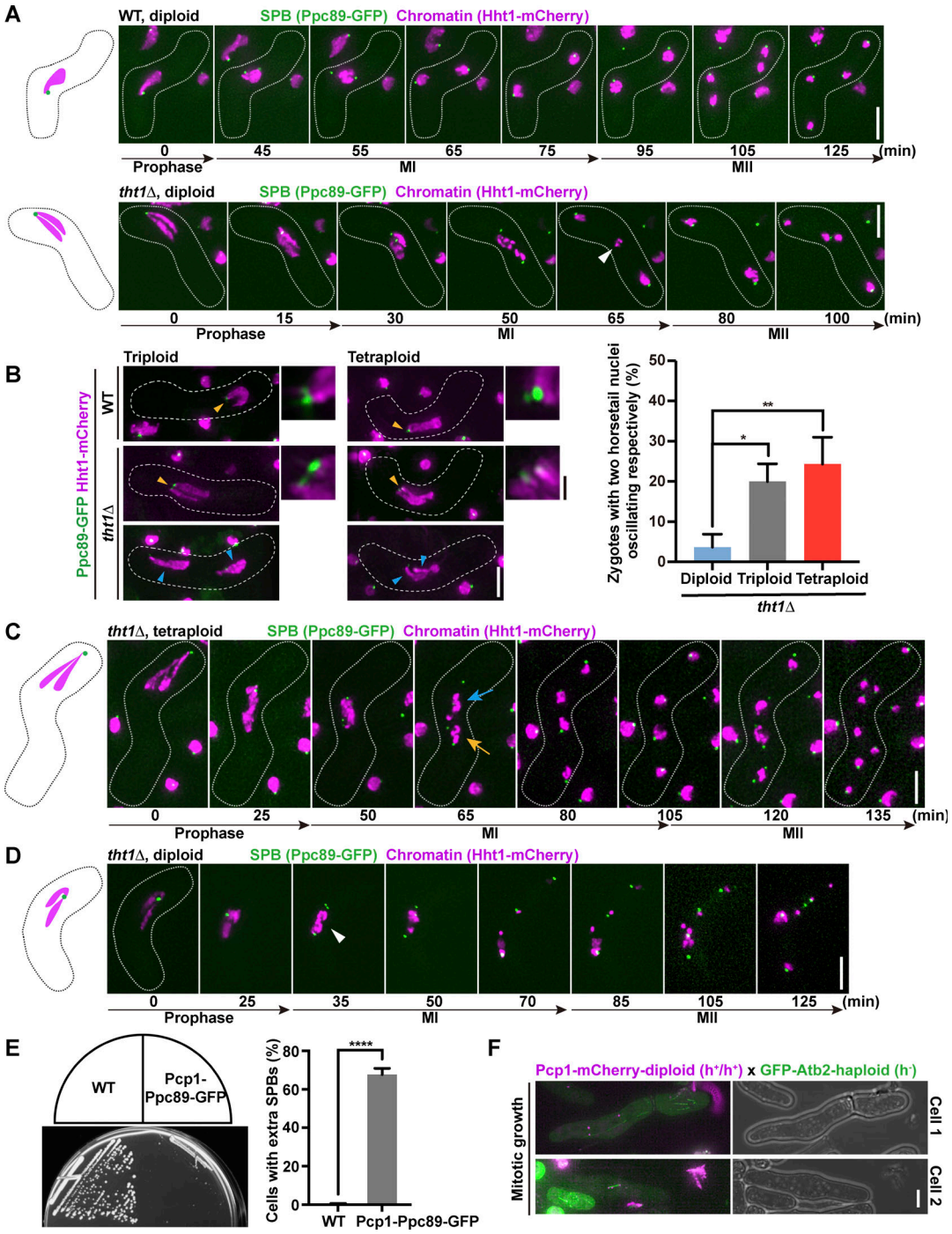

Figure S5. **Blockage of SPB fusion is prone to occur in polyploid zygotic meiosis. (A)** Representative time-lapse images of WT (upper panels) and *tht1Δ* (lower panels) diploid zygotes expressing Ppc89-GFP (SPB) and Hht1-mCherry (chromatins). Arrowhead points to a nuclear division defect in the *tht1Δ* diploid zygote. **(B)** Representative microscopic images of horsetail stage in WT or *tht1Δ* polyploid zygotes expressing Ppc89-GFP (SPB) and Hht1-mCherry (chromatins; left panels). Blue arrowheads point to two unfused horsetail nuclei oscillating separately. Yellow arrowheads point to two adjoining SPBs. SPBs indicated by yellow arrowheads are enlarged in insets. Quantification of zygotes with two unfused horsetail nuclei oscillating separately in the indicated ploidy (right panels). Error bars are SDs from three independent experiments ($n \geq 200$ cells each). *, $P < 0.05$; **, $P < 0.01$ (one-way ANOVA with Tukey's multiple comparisons test). Scale bars: white, 5 µm; black, 1 µm. **(C)** Representative time-lapse images of *tht1Δ* tetraploid zygotes expressing Ppc89-GFP (SPB) and Hht1-mCherry (chromatins). Arrows point to unfused nuclei undergoing meiosis separately. **(D)** Representative time-lapse images of *tht1Δ* diploid zygotes with supernumerary SPBs. Arrowhead points to extra SPBs at MI. **(E)** A single colony formed by the mitotic proliferation of diploid zygote from the mating of two WT gametes or the mating of two gametes expressing Pcp1–Ppc89–GFP was streaked on a YES plate and incubated at 29°C for 4 d (left panels). Right panel shows quantification of cells with supernumerary SPBs in the corresponding single colony shown in the left panel. Error bars are SDs from three independent experiments ($n \geq 200$ cells each). ****, $P < 0.0001$ (two-tailed *t* test). **(F)** Representative microscopic images of mitotic growth of zygotes derived from the mating of a diploid gamete expressing Pcp1-mCherry (SPB) and a haploid gamete expressing GFP-Atb2 (microtubules). Scale bar, 5 µm. Time 0 in A, C, and D is an arbitrary time point in horsetail stage. Scale bars, 5 µm.

Provided online are two tables. Table S1 lists yeast strains used in this study. Table S2 lists primers used in this study.